PERFORMANCE ANALYSIS OF AN EXISTING WIND-ASSISTED COMBINED POWER PLANT

2022
MASTER THESIS
MECHANICAL ENGINEERING

Hasan YASSİN

Thesis Advisor
Assist. Prof. Dr. Abdulrazzak AKROOT

PERFORMANCE ANALYSIS OF AN EXISTING WIND-ASSISTED COMBINED POWER PLANT

Hasan YASSİN

T.C.
Karabuk University
Institute of Graduate Programs
Department of Mechanical Engineering
Prepared as
Master Thesis

Thesis Advisor
Assist. Prof. Dr. Abdulrazzak AKROOT

KARABUK

August 2022

I certify that in my opinion the thesis submitted by Hasan Yassin titled "PERFORMANCE ANALYSIS OF AN EXISTING WIND-ASSISTED COMBINED POWER PLANT" is fully adequate in scope and quality as a thesis for the degree of Master of Science.

Assist. Prof. Dr. Abdulrazzak AKROOT .....
Thesis Advisor, Department of Mechanical Engineering

This thesis is accepted by the examining committee with a unanimous vote in the Department of Mechanical Engineering as a Master of Science thesis. 10.08.2022

Examining Committee Members (Institutions)	Signature
Chairman : Prof. Dr. Yaşar YETİŞKEN (KBU)	.....
Member :Assist. Prof. Dr. Abdulrazzak AKROOT (KBU)	.....
Member :Assist. Prof. Dr. Muhammet ÖZDOĞAN (OMU)	.....

The degree of Master of Science by the thesis submitted is approved by the Administrative Board of the Institute of Graduate Programs, Karabuk University.

Prof. Dr. Hasan SOLMAZ .....
Director of the Institute of Graduate Programs

"All the information in this thesis has been obtained and presented following academic rules and ethical principles; I further declare that I have made all attributions that do not originate in this work, as required by these rules and principles."

Hasan YASSİN

ABSTRACT

M. Sc. Thesis

PERFORMANCE ANALYSIS OF AN EXISTING WIND-ASSISTED COMBINED POWER PLANT

Hasan YASSİN

Karabük University
Institute of Graduate Programs
The Department of Mechanical Engineering

Thesis Advisor:
Assist. Prof. Dr. Abdulrazzak AKROOT
June 2022, 60 pages

The exhaust gases from a gas turbine (GT) are used in combined cycles to enhance the power produced and the thermal efficiency of the cycle. Typically, 30-40% of the gas turbine shaft effort is utilized to drive the compressor. The current research looks at a system that was created combines wind turbines (WTs) with an integrated gas vapor cycle (GTCC). It shows how WTs may be utilized to power the compressor in the GT cycle and pump fluid through an ideal Rankine cycle to boost total power production and efficiencies of the combined cycle.

Since WT will supply the power needed for the compressor and pump instead of typical energy from the GT, the new system is more flexible than a combined cycle alone. Thermodynamic analysis of a combined cycle (Brayton + Rankine) aided by a

wind turbine is the focus of the current work. This study also looks at how the performance of the recommended system is affected by various operating conditions.

An EES (Engineering equation solving) computer program is programmed to solve a mathematical equation and used to analyze the developed system. According to the investigation and analysis results, 44 units of SWT-DD-130 Siemens wind turbine can cover the power required for both the compressor and pump with a critical wind velocity of 9.9 m/s.

The results presented that the addition of wind turbines (WTs) to the gas turbine combined cycle (GTCC) provides more power output (compared with a GTCC without WTs). Besides, the combined gas turbine cycle produces 193.4 MW, while the WT-GTCC cycle produces 355.4 MW. (This means adding the WTs to the GTCC cycle increases the electricity produced by 162 MW). According to the results, both energy and exergy efficiencies of the existing wind-assisted combined power plant were enhanced by 72.44% and 68.25%, respectively. The highest irreversibility in the wind turbine and the combustion chamber of the WT- GTCC cycle has been discovered as 47.2% and 37.21%, respectively.

Key Words **:** Wind energy, Combined Cycle, Power Plant, Renewable Energy, Exergy efficiency, Energy efficiency.

Science Code : 91436

ÖZET

Yüksek Lisans Tezi

RÜZGAR DESTEK İLE KOMBİNE ENERJİ SANTRALİN PERFORMANS ANALİZİ

Hasan YASSİN

Karabük Üniversitesi
Lisansüstü Eğitim Enstitüsü
Makina Mühendisliği Anabilim Dalı

Tez Danışmanı:
Dr. Öğretim Üyesi Abdulrazzak AKROOT
Ağustos 2022, 60 sayfa

Gaz türbininden (GT) çıkan egzoz gazları, üretilen gücü ve termal verimliliği artırmak için kombine çevrimlerde kullanılır. Tipik olarak, gaz türbini şaftının %30-40'ı kompresörü çalıştırmak için kullanılır. Mevcut araştırmadaki, rüzgâr türbinlerini (WT'ler) entegre gaz buharı döngüsünü (GTCC) birleştirerek oluşturduğu sisteme bakmaktadır. GT çevriminde kompresöre güç sağlamak ve kombine çevrimin toplam güç üretimini, verimliliğini artırmak için ideal bir Rankine çevrimi aracılığıyla sıvıyı pompalamak için RT'lerin nasıl kullanılabileceğini göstermektedir.

WT, GT'den gelen tipik enerji yerine kompresör ve pompa için gereken gücü sağlayacağından, yeni sistem tek başına kombine çevrimden daha esnektir. Bir rüzgar türbini tarafından desteklenen kombine çevrimin (Brayton + Rankine) termodinamik analizi, mevcut çalışmanın odak noktasıdır. Bu çalışma önerilen sistemin performansının çeşitli çalışma koşullarından nasıl etkilendiğini de incelemektedir.

Matematiksel bir denklemi çözmek için EES (Mühendislik denklemi çözme) bilgisayar programı programlanmakta ve geliştirilen sistemi analiz etmek için kullanılmaktadır. Araştırma ve analiz sonuçlarına göre 44 adet SWT-DD-130 Siemens rüzgâr türbini, 9,9 m/s kritik rüzgâr hızı ile hem kompresör hem de pompa için gereken gücü karşılayabilmektedir.

Sonuçlar, gaz türbini kombine çevrimine (GTCC) ve rüzgâr türbinlerinin (WT'ler) eklenmesinin daha fazla güç çıkışı sağladığını göstermektedir. (WT'leri olmayan bir GTCC ile karşılaştırıldığında). Ayrıca, kombine gaz türbini çevrimi 193.4 MW, WT-GTCC çevrimi ise 355,4 MW üretmektedir. (Bu, GTCC döngüsüne WT'lerin eklenmesi, üretilen elektriği 162 MW artırdığı anlamına gelir). Elde edilen sonuçlara göre mevcut rüzgâr destekli kombine santralin hem enerji hem de ekserji verimliliği sırasıyla %72,44 ve %68,25 oranında artırılmaktadır. WT- GTCC çevriminin rüzgâr türbininde ve yanma odasında en yüksek tersinmezlik sırasıyla %47,2 ve %37,21 olarak görülmektedir.

Anahtar Kelimeler : Rüzgâr enerjisi, Kombine Çevirim, Güç Santrali, Yenilenebilir Enerji, Ekserji verimliliği, Enerji verimliliği.

Bilim Kodu **:** 91436

ACKNOWLEDGMENT

This humble effort is dedicated to my father and mother, as well as my family, who have always been by my side and supported me throughout my studies and beyond. I shall be eternally grateful to them and may Allah allow me the ability to express my appreciation and thanks to them. Furthermore, I want to sincerely dedicate this work to my advisor, Assist. Prof. Dr. Abdulrazzak AKROOT, who has led and supported me through the most difficult periods, and without him I would not have been able to attain this level and complete this research. Furthermore, I would like to express my gratitude to all the diligent professors and staff members of Karabuk University's engineering faculty.

CONTENTS

Page

Page

Page

LIST OF FIGURES

Page

Page

Page

LIST OF TABLES

Page

SYMBOLS AND ABBREVIATIONS INDEX

SYMBOLS

ρ	: density
T	: temperature
$\dot{m}$	: mass flow rate
P	: pressure
V	: velocity
A	: area
W_a	: maximum theoretical work
$\dot{W}_{WT}$	: total work of wind turbine
W_e	: useful work of wind turbine
W_u	: theoretical work of wind turbine
k_e	: kinetic energy
h	: enthalpy
s	: entropy
EX , X	: exergy
EXd	: exergy destruction
$\dot{S}_g$	: entropy generation
R	: blade radius
ω	: angular velocity
C_P	: power coefficient of wind turbine
ε	: exergy efficiency of wind turbine
λ	: tip speed ratio
k	: gas constant
W	: work

c_p : Specific Heat at Const. Press.

Ψ : Exergy efficiency

Q : Heat

n : number of unit wind turbine

MW : Molecular weight

ch : Chemical exergy

ABBREVIATIONS

LHV : Lower Heating Value

WT-GTCC : Wind Turbine assisted Gas Turbine Combined Cycle

GTCC : Gas Turbine Combined Cycle

HRSG : Heat Recovery Steam Generation

CC : Combustion Chamber

PART 1

INTRODUCTION

1.1. INTRODUCTION

As worldwide energy consumption has increased, so has research into improving and creating energy extraction and performance enhancement techniques. In conjunction with a gas-vapor combined cycle, wind turbines can be used to save energy produced from turbines in a combined cycle, typically used to power both the pump and the compressor. However, in our present system, the pump and the compressor will be powered by wind turbine energy, and all situations will be explored.[1]

Having typically combined cycle and wind-assisted Combined Power Plant comparison in figure 1-1 saving the Compressor energy is generally driven by 30–40% of the gas turbine shaft effort on Brayton cycle via wind energy and saving it on net produced power also saving the pump energy on Rankine cycle is driven by produced power from turbines via wind energy that will give us higher overall efficiency and higher work.[1]

Wind turbine energy is defined as renewable energy inspired by natural resources that are constantly renewed and non-exhaustible, and classified as unconventional and are pure, inexhaustible, unlimited, and environmentally beneficial energy sources that are characterized by not releasing chemical wastes harmful to the environment.

The introduction of combined cycle plants has been an advancement in the hunt for improved thermal efficiency in traditional power plants. As a result, gas turbines devoted to combined-cycle applications are being developed, which has generated a lot of attention recently.

The importance of power production by gas turbines lies mainly in low initial costs, great dependability, and flexibility in operation. The economics of electricity generation using gas turbines are becoming increasingly more appealing. Another distinguishing feature of gas turbine power plants is their ability to start rapidly and use a variety of fuels, ranging from natural gas to residual oil or powdered coal. Significant advancements in combined cycles have been made in three areas: raising the unit capacity of gas turbine units and improving efficiency Gas turbine facilities are now frequently used to meet peak demand, baseload, and standby power plants.

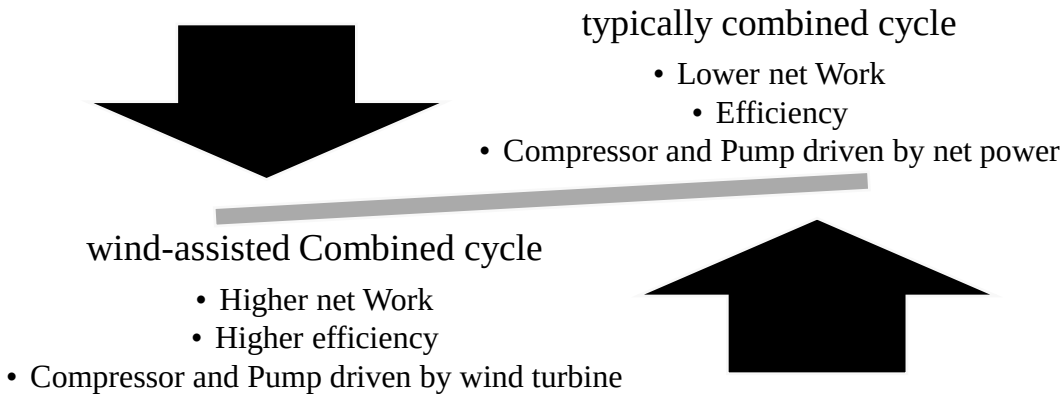

Figure 1. 1. Typically and wind-assisted combined cycle comparison.

1.2.WIND ENERGY

It is a source of renewable energy based on the wind that is available in high altitudes that can bring with fans have 2 or 3 blades fixed on high rods that rotate because of wind, with the axis of rotation aligned with the direction of the wind.

Wind turbines convert wind energy into electricity by using the rotor blades' aerodynamic force, which functions similarly to an airplane wing or helicopter rotor blade. When the wind blows across the blade, the air pressure on one side decreases. Lift and drag are caused by the difference in air pressure between the blade's two surfaces. The rotor rotates because the lift force is greater than the drag force. If the turbine is a direct drive turbine, the rotor is linked to the generator directly. If not, the connection is made through a gearbox, which speeds up rotation and enables the use of a smaller generator. Energy is produced as a result of this conversion of aerodynamic force to generator rotation [3].

1.2.1. Components and Mechanisms of Wind Turbine

- Wind turbine energy extraction depends on wind velocity that creates kinetic energy when wind creates movement on blades.
- The turbine is the foundation stone of a wind energy system; improving or analyzing the performance of a wind energy system depends on the turbine.
- The rotor, major bearing, main shaft, gearbox, and generator compose the drivetrain of a turbine with a gearbox. The drivetrain turns the turbine's rotors (blades, and hub assembly) low-speed, high-torque revolutions into electrical energy.
- Most turbines feature three blades, which are generally constructed of fiberglass. The turbine blades vary, but a typical contemporary land-based wind turbine has blades more than 170 feet long (52 meters). The largest offshore wind turbine is GE's Haliade-X, which has blades 351 feet (107 meters) long — roughly the length of a football field [2]. The air pressure on one side drops when the wind blows across the blade. The differential creates lift and drags air

pressure between the blade's sides. The rotor rotates because the lift force is greater than the drag force.

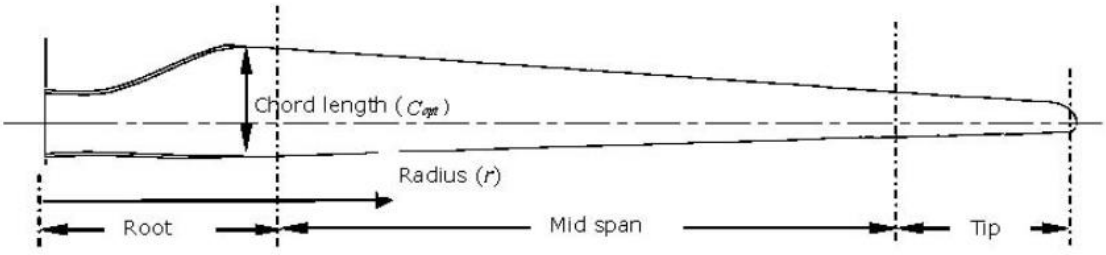

Figure 1. 2. A typical blade layout and grouping of sections [3].

- The blade has several airfoil cross-sections of different sizes and shapes from the root to the tip, developed and designed to capture and streamline the wind during airfoil.
- The critical point for wind turbine the placement that must select a location to maximize the electricity produced from wind turbines because taller towers allow turbines to catch more energy and create more power since wind velocity rises with height. Winds of 30 meters (about 100 feet) or higher are likewise less turbulent.
- That makes a lift force produced when the wind moves over the airfoil, and the wind turbine achieves the basic rotation that makes rotational movement on the rotor that consists of blades and a hub.
- The rotor spins when winds make the rotation; it rotates on an axis parallel to the ground because wind turbine blades generally revolve at a meager rate of revolution per minute owing to mechanical failures. They cannot create any measuring electricity frequency from a generator.
- A gearbox is required before connecting to the generator, which converts mechanical energy into electricity. The gearbox is used to transmit torque by slow-rotating the main shaft and using its gearbox arrangement to achieve the high-speed ratio in the second shaft, which drives the generator—
- preferred to put two generators, a small one for light winds and a big one for strong winds.

- There is a large disk (brake) on the major shaft to shut off torque transferred to the generator. A mechanical mechanism controls the pitch of the blades, so pitch adjustment can also be used to avoid the operation of the turbine under storm conditions. A hydraulic system drives the pitch mechanism, with oil as the shared medium. This system needs servicing and continuous pressure control almost annually, along with the oil-lubricated gearbox. The oil would be treated and must be cooled, leading to mechanical losses in the gearbox.
- Consequently, the electricity passes through the cables towards the base where a step-up transformer is situated.[2]

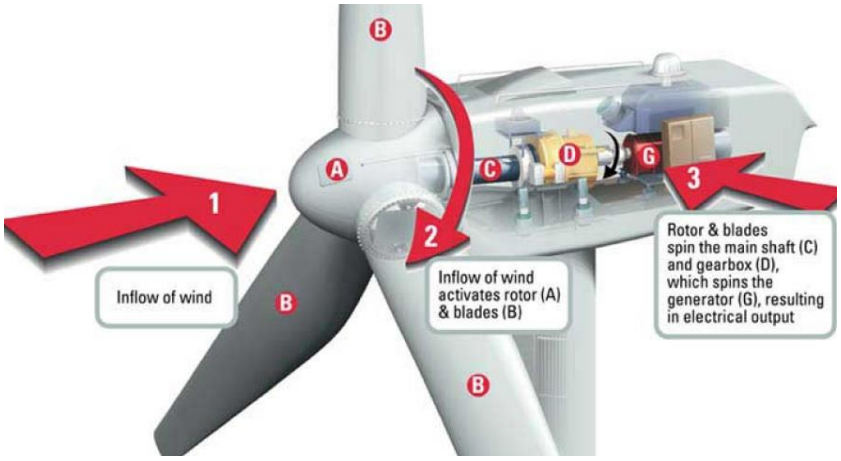

Figure 1. 3. Mechanisms of action [4].

1.2.2. Performance and Evaluation of The Wind Turbines

The turbine is a conversion device of wind energy to mechanical energy that will with blades that capture wind movement that can make a rotary motion on a generator after making organized by the gearbox to produce an electrical energy.

Wind turbine performance and evaluation mainly depend on internal factors (rotor size, blade design, numbers of blades, and generator) externally (placement of wind turbine, wind velocity, and weather).

- Rotor Size: the diameter of the motor constitutes the main point on the efficiency of a wind turbine that affects rotor rotation velocity.

- Blades Number: standard is three for wind turbines, and any wind turbine with more than three blades will slow on generator and wind resistance, making less energy.
- Blade's design and cross-section: it will capture winds that will make the rotation and starting point for the system, so it must design carefully and after making studies on blade shape resistance of wind and how much appears to streamline the wind with its shape.

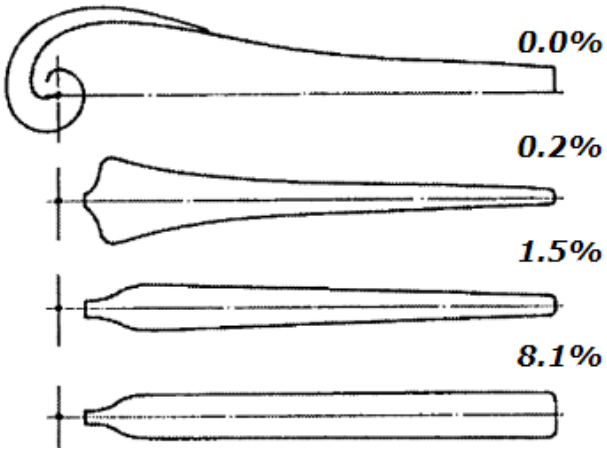

Figure 1. 4. Efficiency losses due to optimal chord length simplification [5].

- The elevation and position of wind turbines, as they are high from the ground, will make more energy.
- Amount of losses power on gearbox (gearbox friction, bearing losses) and generator losses.[6]

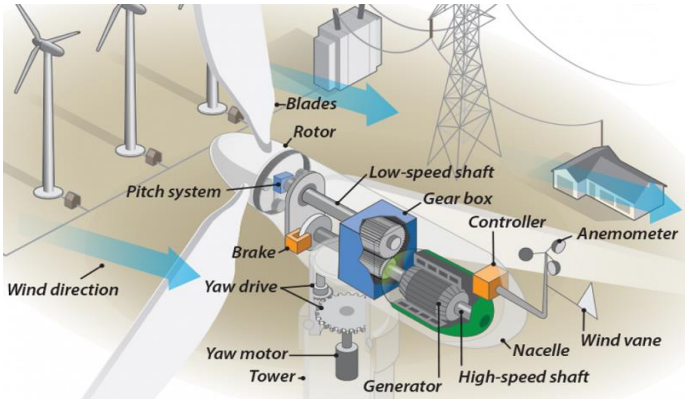

Figure 1. 5 Wind Turbines components [2].

1.2.3. Yaw Mechanisms

When the turbine is running, the electronic controller activates the yaw mechanism by checking the position of the wind vane on the turbine numerous times per second.
For optimum power production, the blades will typically face the wind, but at any moment, the direction of the wind will change.

When the wind has a deviation in the direction, a velocity sensor on the top of the nacelle that measures the wind velocity and direction is sent to an electronic controller signal. This in turn sends a signal to the yawing mechanisms to correct the direction; thus, the wind turbine will always be aligned with the wind direction.[7]

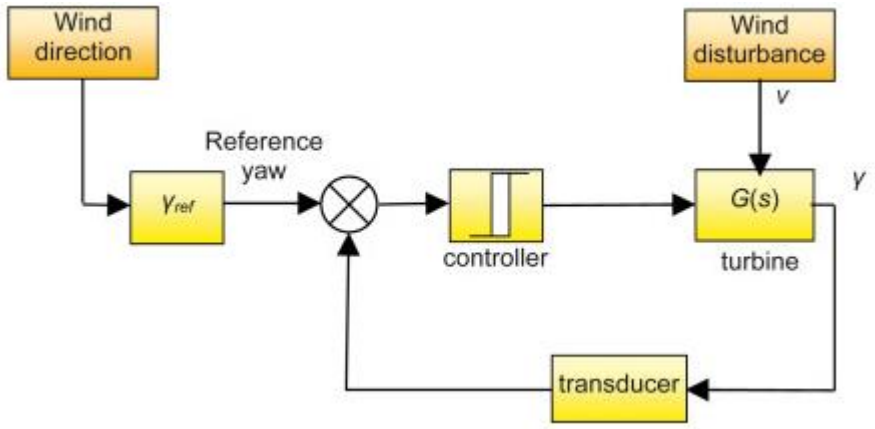

Figure 1. 6. Simple dead-band controller of yaw mechanisms [7].

1.2.4. Pitch System

The pitch system regulates the rotor speed by adjusting the angle of the wind turbine's blades regarding the wind. The pitch mechanism determines the amount of energy the turbine blades can extract by changing the angle of the blades. The pitching system can also make the blade a "feather" and change the angle so that it does not generate enough force to rotate the rotor. If the wind speed is too fast to operate safely, the blade deflection will slow down the turbine's rotor, preventing damage to the equipment [3].

1.2.5. Transformers

Transformers take alternating current (AC) power at one voltage and adjust it to supply electricity as needed. A step-up transformer is used in a wind power plant to boost the voltage (thus lowering the needed current), which reduces the power losses that occur while transporting large quantities of electricity over long distances via transmission lines. When the electricity reaches a neighborhood, transformers decrease the voltage to make it safe and usable by the community's buildings and residences.[2]

1.2.6. Wind Power Plants

Two or more wind turbines are called wind power plants, place of wind power plants must consider the terrain often it is grouping in:

- flat lands in long parallel rows
- hilltops or Open land in long rows
- Dams and drainage channels in Parallel linear arrays.

It is like a traditional power plant with many independent generators (wind turbines) feeding an energy-consuming source; usually, it is a public electricity grid and connects to the main monitoring network [7].

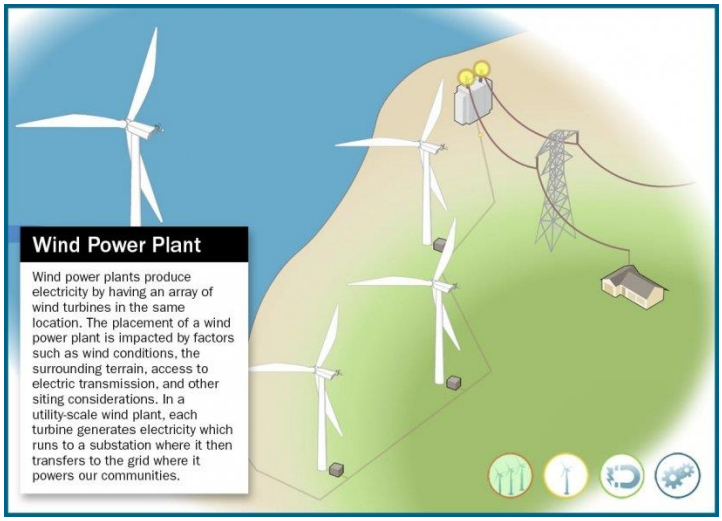

Figure 1. 7. Wind Power Plant [2].

1.3. COMBINED BRAYTON AND RANKINE CYCLE

The pursuit of improved thermal efficiency has resulted in inventive changes to traditional power plants. The combined gas–vapor cycle, or simply the combined cycle, is a more common variant that combines a gas power cycle with a vapor power cycle. The most interesting is the gas-turbine (Brayton) cycle operating at high temperatures atop a steam turbine (Rankine) cycle operating at low temperatures. The gas turbine's high-temperature exhaust gases heat the steam. By converting the exhaust gas into steam, energy is recovered from the exhaust gas, taking advantage of the highly desirable properties of high-temperature gas turbine cycles. It makes sense for researchers to use high-temperature exhaust gases as a source of power for bottoming cycles such as steam-powered cycles [8].

1.3.1. Combined Cycle Description and Components

The Brayton cycle is created from an air compressor that makes an isentropic compression process and combustion chamber that provides heat input with constant pressure, and a gas turbine that makes an isentropic expansion process the thermal efficiency of a Brayton cycle depends and increases with both of these parameters on the pressure ratio of the gas turbine and the specific heat ratio of the working fluid., The exhaust of the Brayton cycle at high temperature and low pressure is used to power a Rankine cycle through cooling heat exchanger is used to reject heat and high and low-pressure steam turbines that make isentropic expansion process and condenser is used to reject heat and finally pump that make Isentropic compression process, boost a power cycle's thermal efficiency by increase the average temperature at which heat is delivered to the boiler's working fluid or reduce the average temperature at which heat is rejected from the condenser's working fluid. That is, during heat addition, the average fluid temperature should be as high as feasible, while during heat rejection, it should be as low as possible.[8]

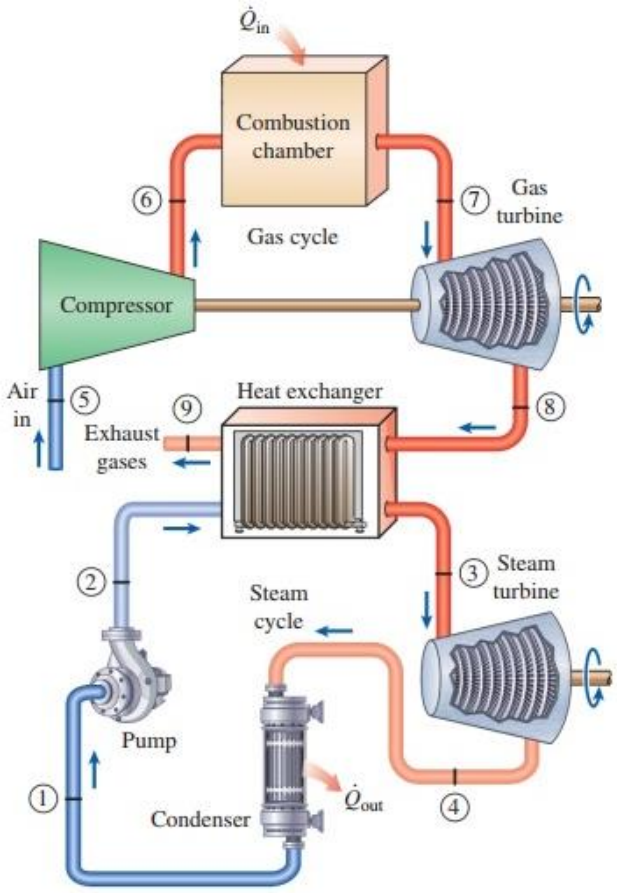

Figure 1. 8. Components of Combined Brayton and Rankine Cycle [8].

The combined cycle uses the same input energy, but it produces more work (by the work of the Rankine cycle steam turbine). The following figure is a schematic of the total heat engine, which may be considered a collection of higher and lower heat engines. The top engine is a gas turbine (Brayton cycle) that transfers heat to the lower engine, a steam turbine (Rankine cycle) [9].

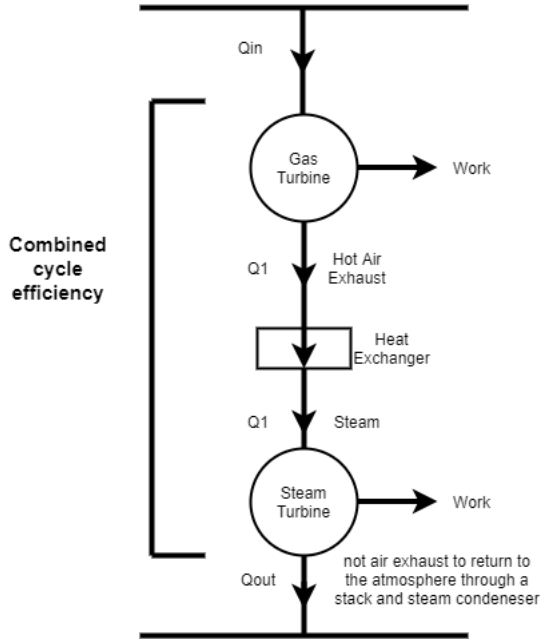

Figure 1. 9. Combined Brayton and Rankine Cycle efficiency [9].

1.3.2. The Overall Efficiency of The Combined Cycle

A combined-cycle power system's overall electrical efficiency is generally in the region of 50–60 percent, which is a significant improvement over the efficiency of a basic, open-cycle application of roughly 33 percent [11].

It is possible to derive it as follows. The heat absorbed by the gas turbine is denoted as $\dot{Q}_{in}$, while the heat rejected to the atmosphere is denoted as $\dot{Q}_{out}$. $\dot{Q}_1$ denotes the heat emitted by the gas turbine.[10]

The hot exhaust gases from the gas turbine flow via a heat exchanger and are utilized as a heat source for the two-phase Rankine cycle, resulting in Q 1 being the heat input to the steam cycle as well. In other words, the gas turbine's heat input powers both the gas and steam cycles.

This is how a combined-cycle plant generates electricity and absorbs waste heat from the gas turbine to improve efficiency and output.

1. The gas turbine consumes fuel: The gas turbine compresses air and combines it with fuel that has been heated to extremely high temperatures, the spinning of the gas turbine blades is caused by the hot air-fuel combination moving through them, the rapidly rotating turbine powers a generator, which turns some of the spinning energy into electricity.

2. A heat recovery system captures exhaust: A Heat Recovery Steam Generator (HRSG) collects gas turbine exhaust heat that would otherwise escape via the exhaust stack, the HRSG generates steam from the exhaust heat of the gas turbine and delivers it to the steam turbine

3. The steam turbine generates additional electricity: The steam turbine's energy is transferred to the generator drive shaft, where it is turned into more electricity [13].

1.4. SUMMARY

The current running models of the combined power generation cycles, especially (Brayton Rankine), dismiss approximately 30% of the total power used as input power to the compressor and pump. The thermal efficiency of combined power generation cycles can be dramatically enhanced by utilizing input power to the compressor and pump from wind turbines.

Because of their efficiency, CCGTs have become a cornerstone of generating fleets in the United States, the United Kingdom, and other nations. Since 2000, the United States has installed 267 GW of CCGT capacity, with CCGTs accounting for 56% of gas-fired generating capacity [11]. In the United States, gas substitutes coal, increasing the average CCGT capacity factor from around 35 percent in 2005 to over 60 percent [15], and by assisted wind combined cycles, the efficiency will wide increase. However, they must overcome several obstacles before may implement these ideas.

1.5. THESIS OBJECTIVES

This project aims to model, analyze, and simulate the wind-Assisted combined power plant generation system. Study effect of design parameters, the impact of mechanical consideration of wind velocity, exergy parameters, and efficiency. The main objectives of this research are summarized as follows:

1. Design and model a wind-assisted combined power generation cycle.
2. Create a computer program using EES software to analyze the performance and simulate a wind-assisted combined power generation cycle couple.
3. Investigate the effect of different operating conditions on the performance of the horizontal axis wind turbine.
4. Investigate the effect of different operating conditions on the performance of the developed system.

PART 2

LITERATURE REVIEW

2.1. INTRODUCTION

There is a wealth of literature devoted to the modeling, design, and study performance of combined gas–vapor cycle and wind power plants and their applications due to the importance of renewable energy.

The world is working to develop and increase renewable energy because of environmental and economic advantages compared to conventional energies. Therefore, it should remain in continuous and permanent development.

This chapter will include past work on energy flow, modeling, optimization approaches, and control technologies for Wind turbines and combined gas–vapor cycles. It also presents and invests a list of literature reviews on combined gas–vapor cycle and wind power plants.

2.2. WIND ENERGY CONVERSION SYSTEM

Wind power is estimated to be 3.6*109 MW around the globe; however, precise estimations from the World Meteorological Organization show that only 1% of wind power is accessible for energy exploitation in diverse places and is expected to be roughly 0.6Q (175*1012 KWh) [16]. Also, A wind turbine's rotation speed is determined by its aerodynamic characteristics and the size of its wind blades. Furthermore, the turbine's connection to the electric grid is critical since all modern wind generators that are linked to the grid produce electric current with the same frequency as the central grid.

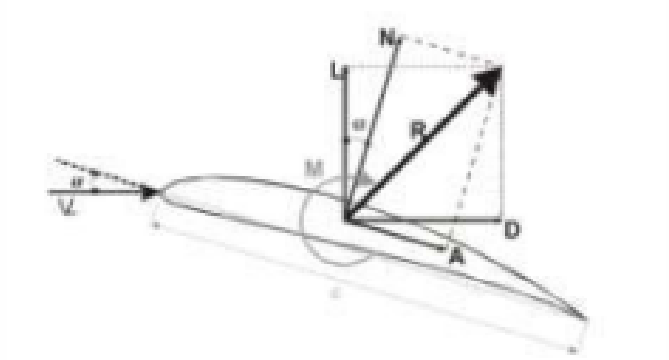

Figure 2. 1. The resulting aerodynamic force and its constituents [12].

The net driving force will rise if the reverse force on the returning blade is decreased. The deflector plate enhances the power coefficient by 50% when it is in its ideal position, according to Golecha's [17] results. The highest power coefficient in the presence of a deflector plate is 0.21 at a tip speed ratio of 0.82. The maximum coefficient of power for a three-stage modified Savonius rotor, a two-stage 0° phase shift, and a 90° phase shift with a deflector plate improve by 42%, 31%, and 17%, respectively.

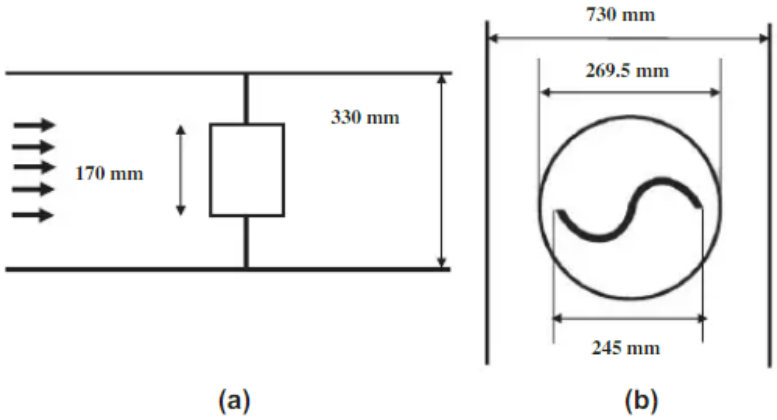

Figure 2. 2. (a) view of the experimental setup and channel from the side. (b) the experimental setup channel from above [13].

Using computational methods, Mohamed et al. [18] improved the shape and location of a flat deflector for two- and three-blade Savonius turbines. Both turbines saw a 27% increase in performance, even though the deflector's optimal geometry differed from turbine to turbine.

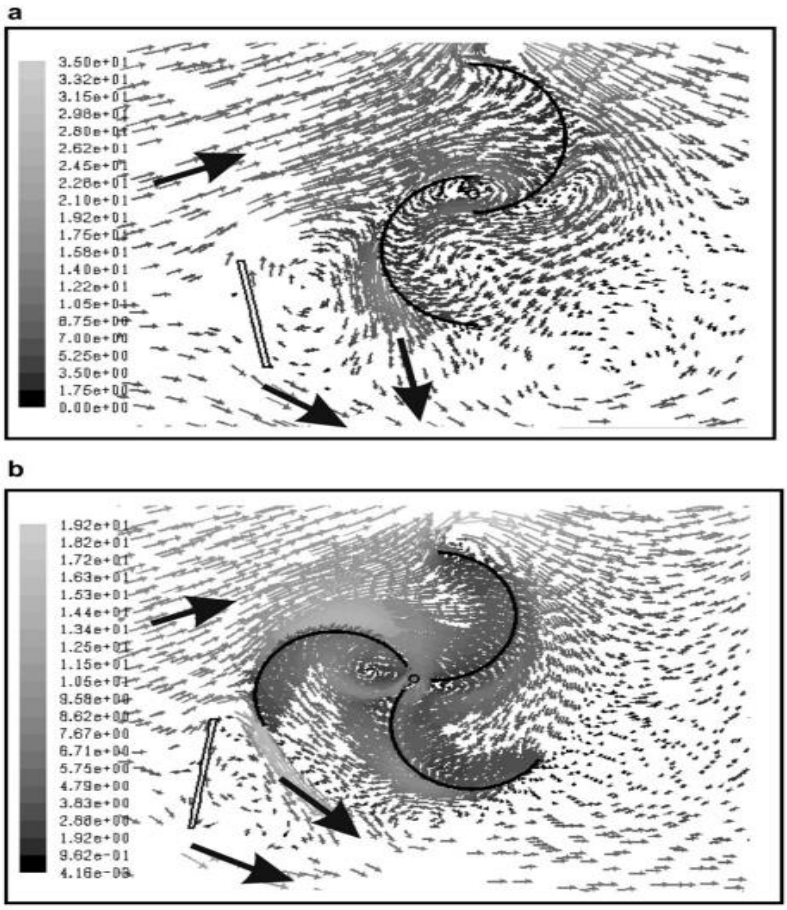

Figure 2. 3. Comparison of instantaneous flow structures with leading blades in vertical position for optimal configuration at $\lambda = 0.7$ a: 2-blade turbine. b: 3-blade turbine [14].

Altan et al. [19] revealed that the power output of a Savonius turbine rose more than double that of a regular turbine because of an efficient arrangement of two deflecting flat plates that guide incoming wind to advancing blades.

For the axis vertical, the circumferential flow of a Savonius wind turbine blade is quantitatively analyzed. For a wind velocity of 6 m/s, three distinct scenarios were applied to the tunnel entrance, yielding three different (0°-45° and 90°) blade angles and vectorial velocity graphs.

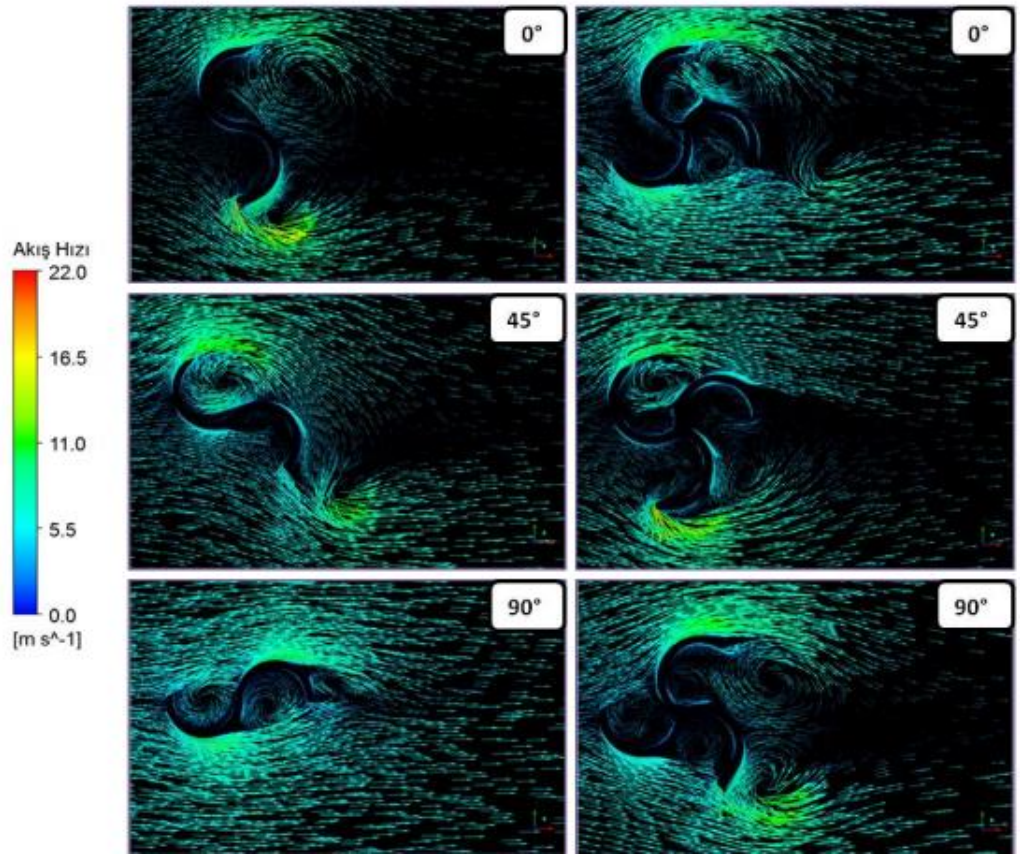

Figure 2. 4. Velocity distributions around the wing [15].

Crawford [16] studied the size and energy yield of WTs in the life cycle energy and greenhouse emission assessments. Comparing two different size turbines shows that, while using a large WT reduces the footprint area per unit of rated power, there is no discernible difference in energy yield between small and large turbines.

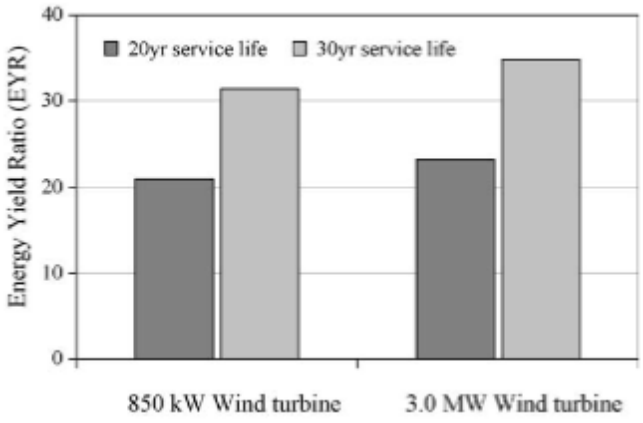

Figure 2. 5. Wind turbines with an energy yield ratio of 850 kW and 3.0 MW [16].

Energy and exergy evaluations of vertical and horizontal WTs were provided by Pope et al. [17]. The results revealed that energy and exergy efficiencies differed by 50-53 percent for horizontal WTs and 44-55 percent for vertical WTs. Improved site selection and turbine design using an exergy technique can also boost WT output capacity while lowering economic costs.

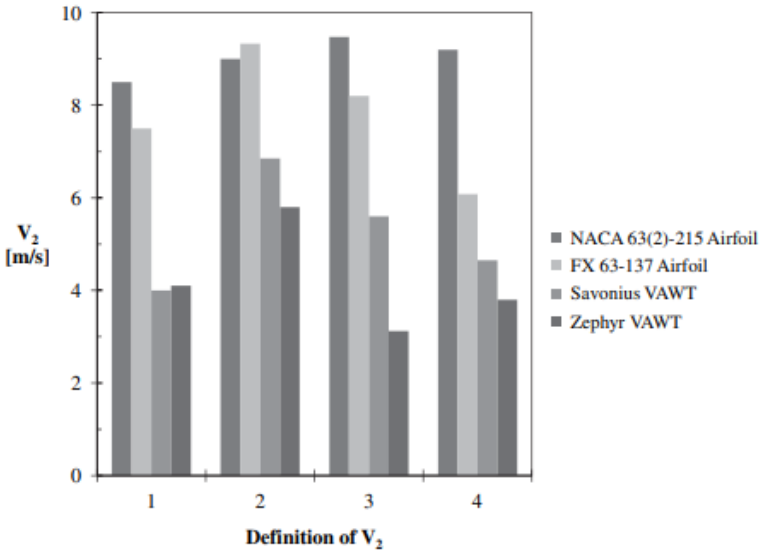

Figure 2. 6. Definitions of velocity for a variety of wind power systems [17].

Hall et al. [18] proposed a variable ratio gearbox in a WT to improve system efficiency. According to the findings, a variable ratio gearbox may benefit all sorts of WTs, independent of their type, and enhance efficiency at a reasonable cost.

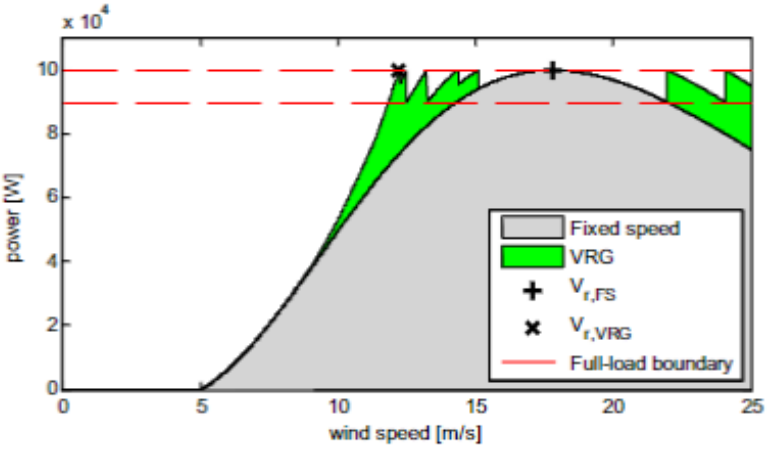

Figure 2. 7. Power curve by using a VRG (Variable ratio gear) [18].

Wind turbines were operated using a nonlinear feedback linearization controller and an Extended Kalman Filter by Kumar and Stol [23]. A LQR was contrasted with the recommended controller (linear quadratic regulator). The proposed controller provided better control over rotor speed regulation when the wind speed was close to the rated wind speed. The controller showed decreases in low-speed shaft fatigue damage equivalent loads, power regulation, and speed regulation compared to a Gain Scheduled Proportional Integral controller created specifically for speed regulation. When the wind speed was close to the rated wind speed, the feedback linearization controller outperformed a LQR but underperformed at higher wind speeds.

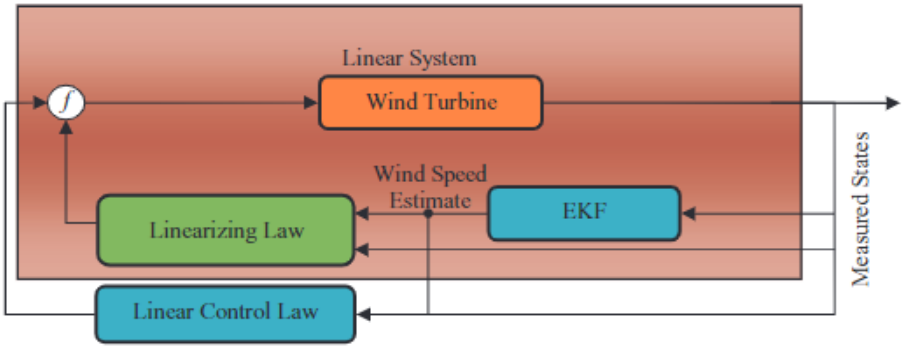

Figure 2. 8. Suggested controller with an extended Kalman filter to operate wind turbines [19].

Wind turbines are subjected to unbalanced effects such as strong winds, which results in variable blade air loads, and performance stress loads can cause damage to turbine components and, ultimately, breakdowns. Shen et al. [24] evaluated wind turbine aerodynamics and loads under wind shear flow, which would result in unstable blade air loads and performance. The turbine blades were modeled using the advanced lifting surface approach with a time marching free wake model. Individual pitch control was used to prevent flap-wise fatigue damage in wind turbine blades and discovered that IPC of the fluctuating blade root flap-wise moment might significantly minimize flap-wise fatigue damage. However, blade root edgewise moments are less susceptible to shifting blade pitch than blade root flap-wise moments.

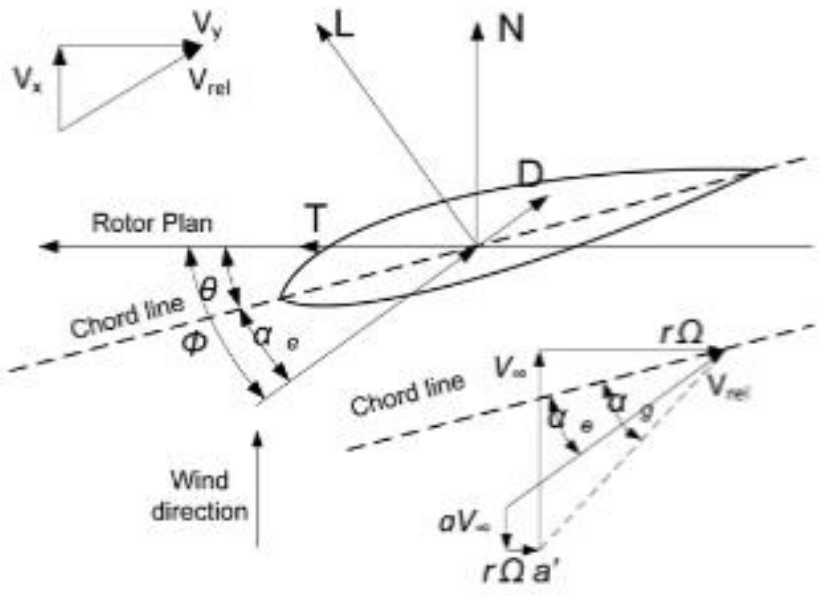

Figure 2. 9. A diagram of a blade element's velocity and force decompositions [20].

2.3. COMBINED GAS–VAPOR CYCLE

The reheat mixed Brayton/Rankine power cycle was investigated by Khaliq et al. [21]. Using the second-law technique, they evaluated the influence of factors such as pressure ratio, cycle temperature ratio, number of reheats, and cycle pressure drop on the combined cycle performance. Their modeling findings revealed that the combustion chamber is the site of the highest exergy destruction.

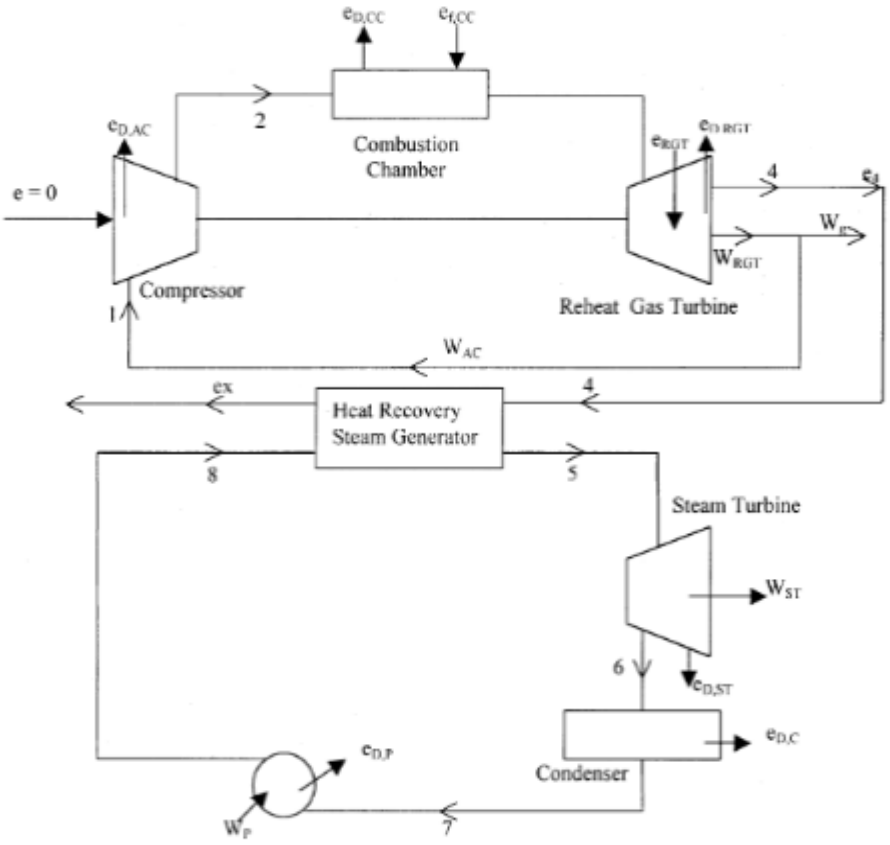

Figure 2. 10. Schematic diagram of the combined Brayton/Rankine power cycle with reheat [21].

Khaljani et al. [26] combined a gas turbine (GT) with an ORC via a single-pressure heat recovery steam generator (HRSG). Through computer modeling, they discovered that raising the pressure ratio and the compressor and gas turbine isentropic efficiencies improved thermodynamic performance while lowering total costs. Furthermore, increasing the departing temperature of the air preheater will benefit the system both thermodynamically and economically. The rise in the condensation temperature and pinch point temperature difference of the ORC evaporator, as well as the increase in the pinch point temperature difference of the heat recovery steam generator, reduces the first and second law efficiency and raises the system's overall cost rates.

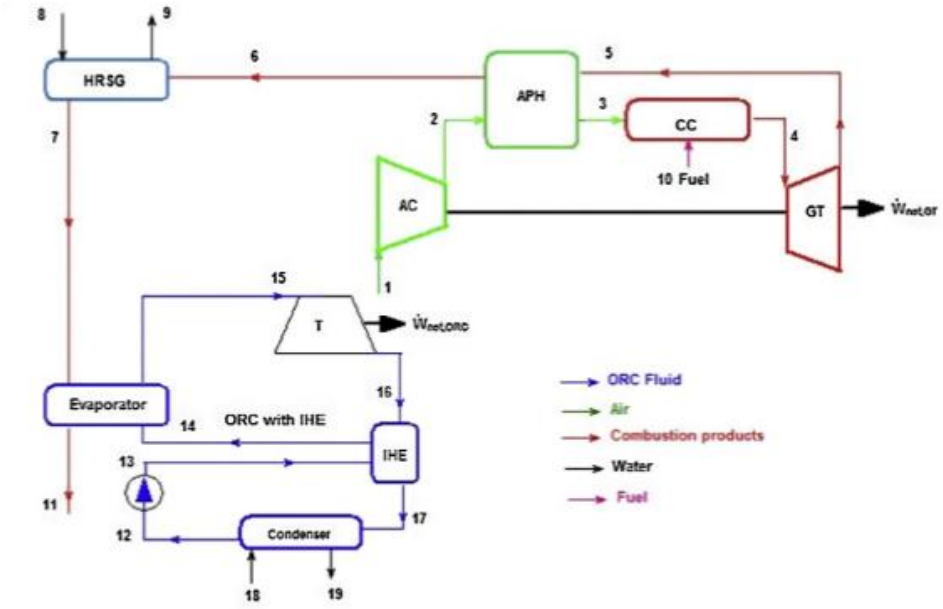

Figure 2. 11. Schematic diagrams of the combined heat and energy of combined gas turbine and organic Rankine cycle [22].

Marrero et al. [23] investigated and improved the exergy processes of integrated triple power plants. The Brayton cycle (gas-based) and two Rankine cycles are examined in the triple analysis (steam and ammonia based). The results revealed that the heat recovery heat exchanger had the highest exergy destruction. Their research indicated that using feedwater heaters increases efficiency. Furthermore, when the ambient temperature rises, exergy efficiency falls, and as pressure rises, the ratio of exergy efficiency rises to a particular level before falling.

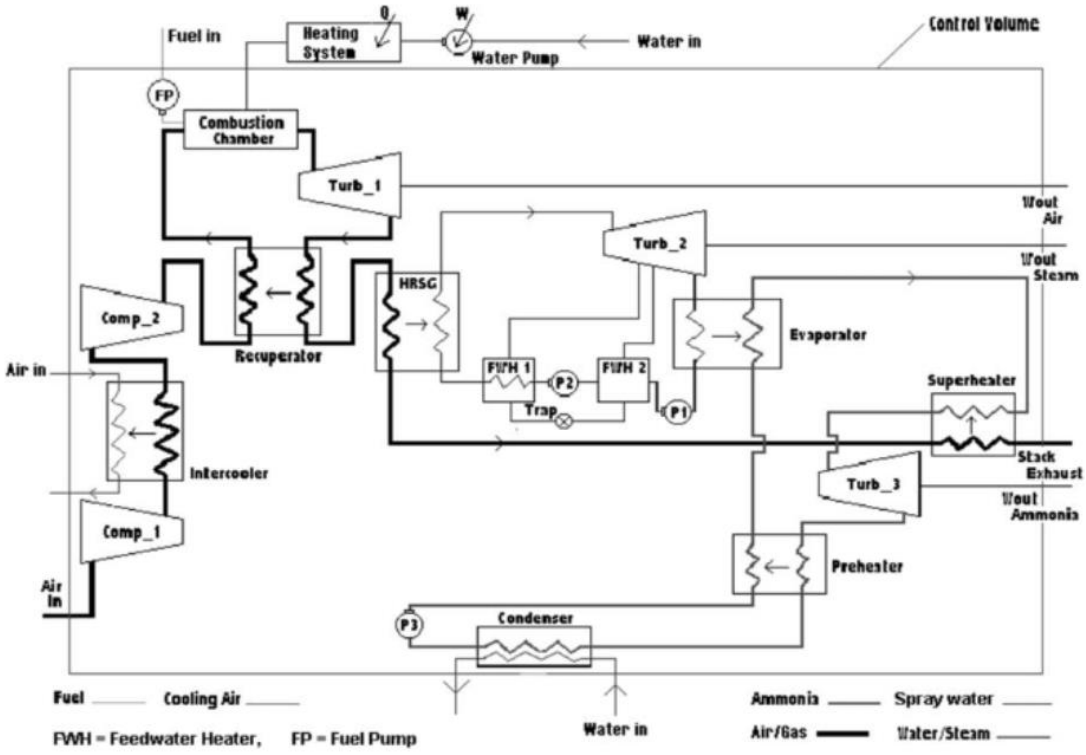

Figure 2. 12. Schematic diagram of the triple cycle [23].

Ahmadi et al. [24] investigated the energy, exergy, exergy-economic, and environmental aspects of a combined power plant as well as the impact of additional firing based on bottoming cycle performance and CO2 emissions. They employed the first and second principles of thermodynamics. The results showed that when the pressure ratio increased, the power of the steam cycle dropped. As a result, the system's total efficiency rose, and CO2 emissions fell. Furthermore, CO2 emissions can be decreased by choosing the optimal component with a low fuel injection rate.

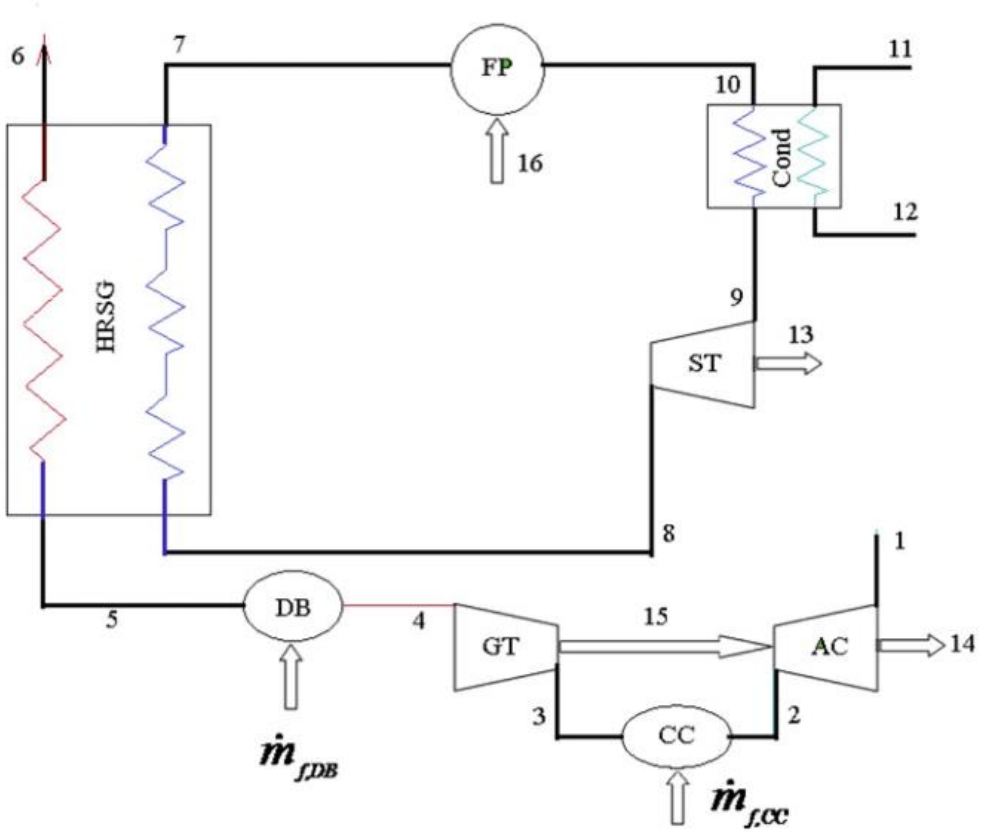

Figure 2. 13. A combined cycle power plant schematic with additional firing [24].

Cihan et al. [25] used a parametric study of several components to conduct an energy exergy analysis of a power plant in Turkey, utilizing data from its operational units and analyzing a complex energy system, and discovering the possibilities for enhancing system efficiency more completely. The data demonstrate that combustion chambers, gas turbines, and heat recovery steam generators (HRSG) are the primary sources of irreversibility, accounting for more than 85 percent of total exergy losses. Also, some constructive and thermal ideas for these devices have been offered to increase system efficiency. And the results showed that the plant components with the largest exergy destruction are the combustion chamber, gas turbine, and heat recovery heat exchanger.

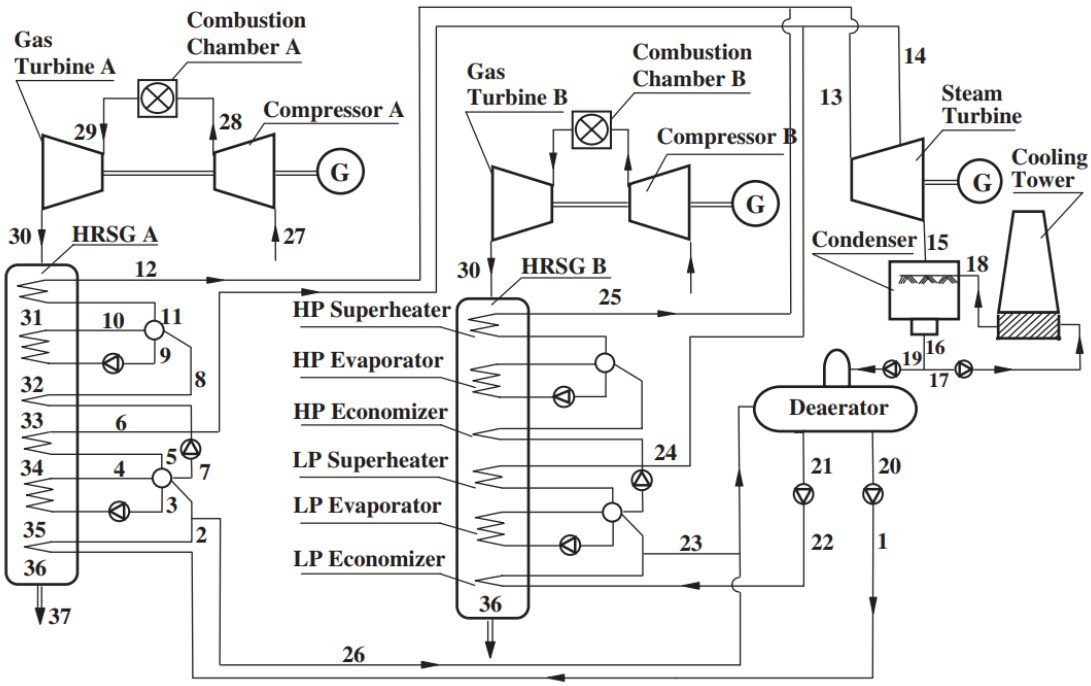

Figure 2. 14. Process schematic for one of the main units of that combined-cycle power plant [25].

Nag et al. [26] proposed using pressured circulating fluidized beds for partial gasification and coal combustion based on the first and second laws. Also, The Redlich-Kwong equation of state is used in the topping gas turbine plant to evaluate the characteristics of air at high pressures. In the bottoming plant, a dual pressure steam cycle is being examined to reduce irreversibility in heat transfer from gas to water and steam, investigated the impact of the gas cycle's pressure ratio and peak cycle temperature ratio, as well as the steam cycle's lower saturation pressure, on the overall performance of the combined plant. Gas turbine working fluid temperatures vary from 1100°C to 550°C, whereas steam turbine working fluid temperatures range from 550°C to the ambient temperature, resulting in close to 50% total efficiency.

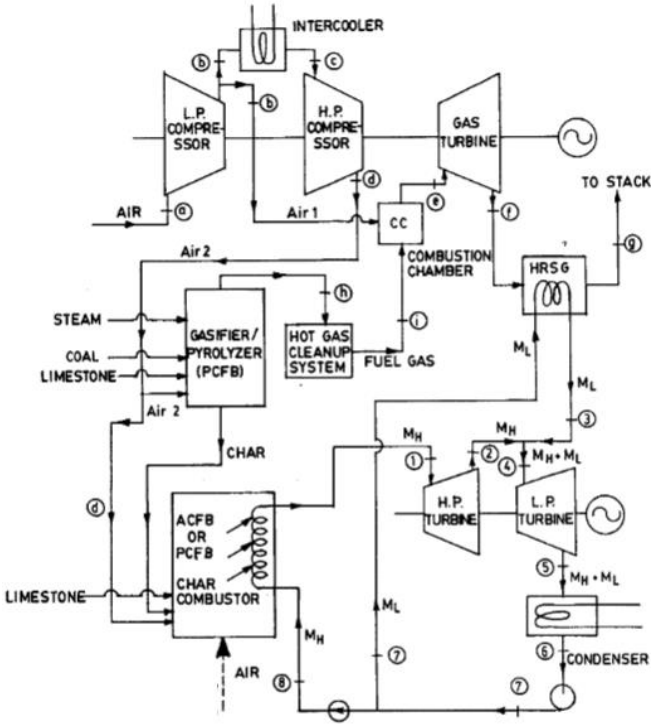

Figure 2. 15. Model of the combined cycle [26].

According to Ibrahim et al. [31], the simple gas turbine configuration is more suited for power production, while the regenerative gas turbine architecture has a greater efficiency regarding ambient temperature. There is little difference in total power output between simple gas turbine and regenerative gas turbine configurations at lower compression ratios because the simple gas turbine has a larger power output at lower compression ratios.

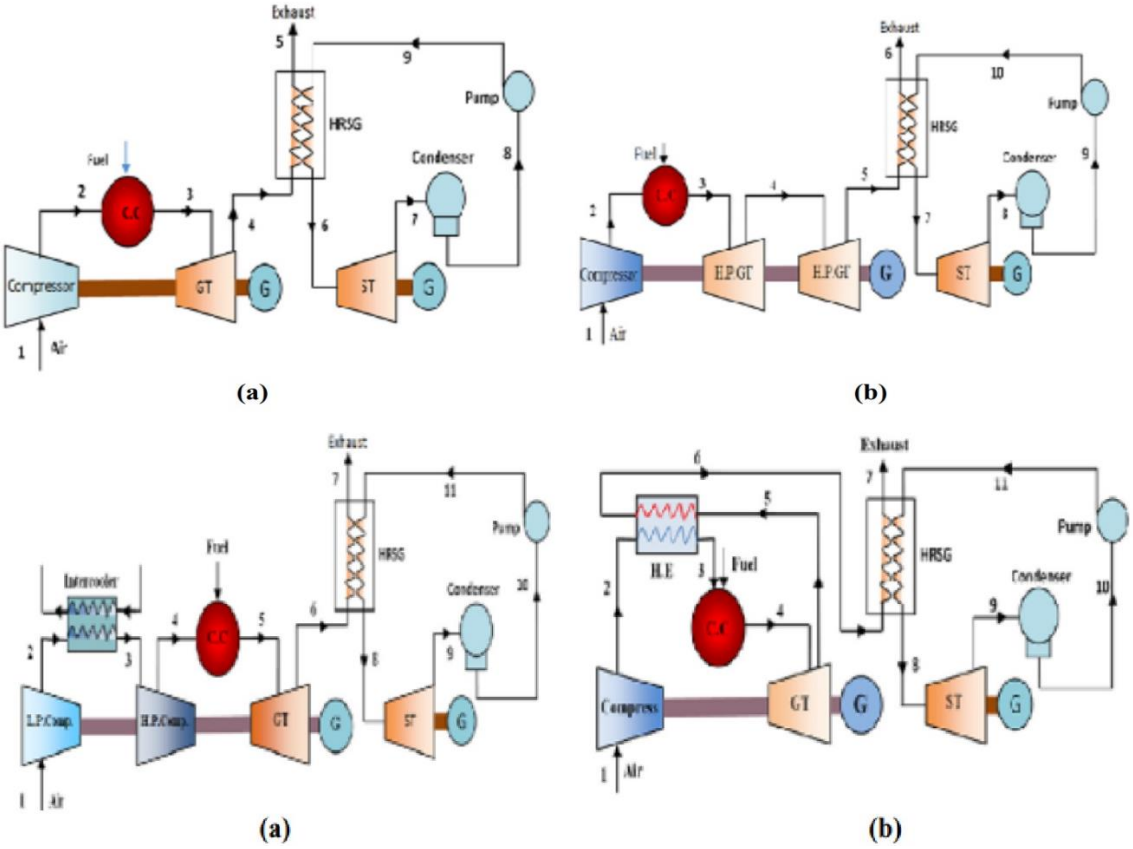

Figure 2. 16. The schematic diagram: a) Simple combined cycle gas turbine power plant b) combined cycle two-shaft gas turbine power plant. a) Intercooler combined cycle gas turbine power plant and Regenerative [27].

Bassily [32] presented a method for reducing the irreversibility of the combined cycle's steam generator. The effects of changing the gas turbine's input temperature (TIT) and pinch points on the performance of all cycles were shown and debated. When the same values of TIT and pinch points are used, the findings show that the optimized combined cycle is up to 1% more efficient than the reduced-irreversibility combined cycle, which is 2–2.5% more efficient than the routinely planned combined cycle.

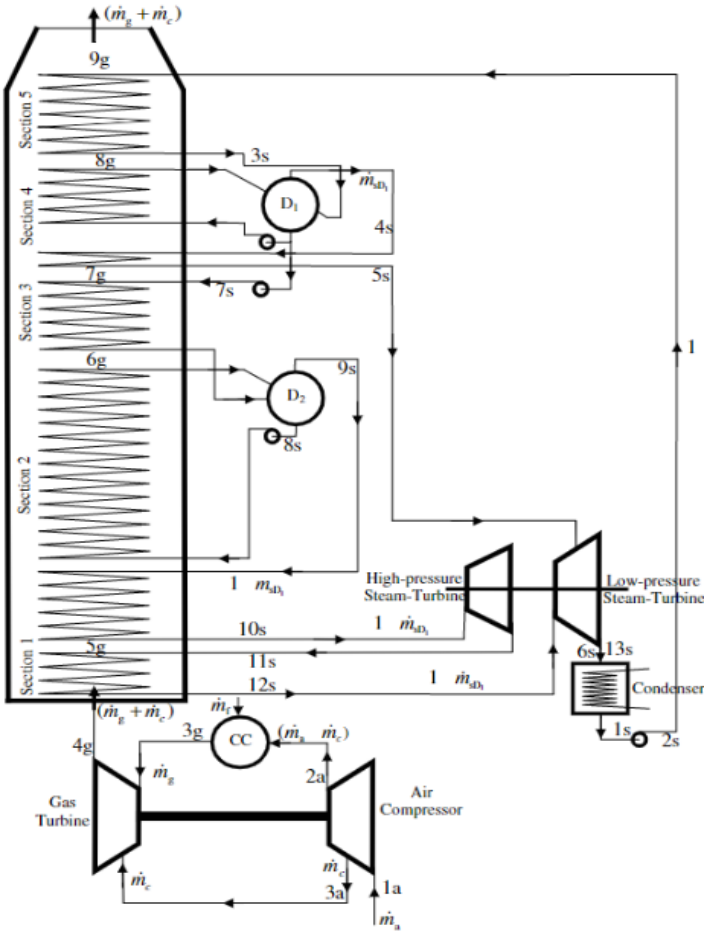

Figure 2. 17. Schematic diagram of the dual-pressure reheats combined-cycle [28].

2.4. WIND TURBINE-BASED COMBINED BRAYTON AND RANKINE CYCLE

Rabbani et al. [1] investigated a combination system consisting of a Wind Turbine (WT) and a combined cycle. Wind energy provided the cycle's necessary energy, calculated based on the quantity of cycle required energy. The load requirement influences the critical velocity and critical mass flow rate. It was necessary to use more wind power to compress air that may be utilized during a low penetration configuration in the case of low demand and high penetration. During periods of high load demand, all the wind power is used to operate the pump and compressor, and the storage unit supplies more compressed air as needed. The calculations show that raising the combustion temperature decreases the critical velocity and mass flow rate. Wind velocity increases diminish the entire system's energy and exergy efficiency.

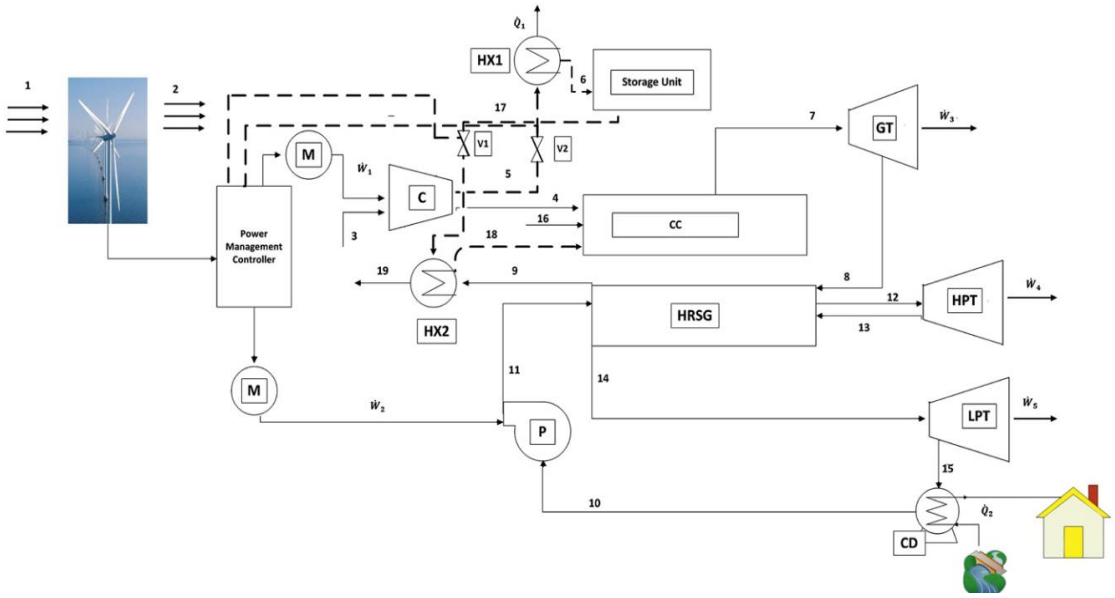

Figure 2. 18. Schematics of the system [1].

Hossein et al. [2] presented complete research on a system that combines a Wind Turbine (WT) with a combined heat and power cycle, with two objective functions of the system's first and second law efficiency. The suggested heat and power combination system in that research contains wind turbines to supply combined cycle electricity, a gas turbine cycle with a capacity of 26 MW, and an ORC to generate additional power. For the assumed base operating circumstances, adding ORC to the system may generate about 273.1 kW more power from waste heat recovery of GT cycle exhaust gases. Wind power is utilized to power the pump and compressor; if necessary, more power is stored by the storage unit, which enters the system when the wind velocity is low. The study's parametric analysis results reveal that increasing the isentropic efficiencies of the air compressor and gas turbine, as well as the gas turbine input temperature, enhances the system's thermodynamic performance. The total system's energy and exergy efficiencies decrease as the wind velocity and compressor pressure ratio increase. Exergy study revealed that the combustion chamber has the largest exergy destruction, the compressor and gas turbine have substantial exergy destruction, and the pump of the organic Rankine cycle has the least exergy destruction.

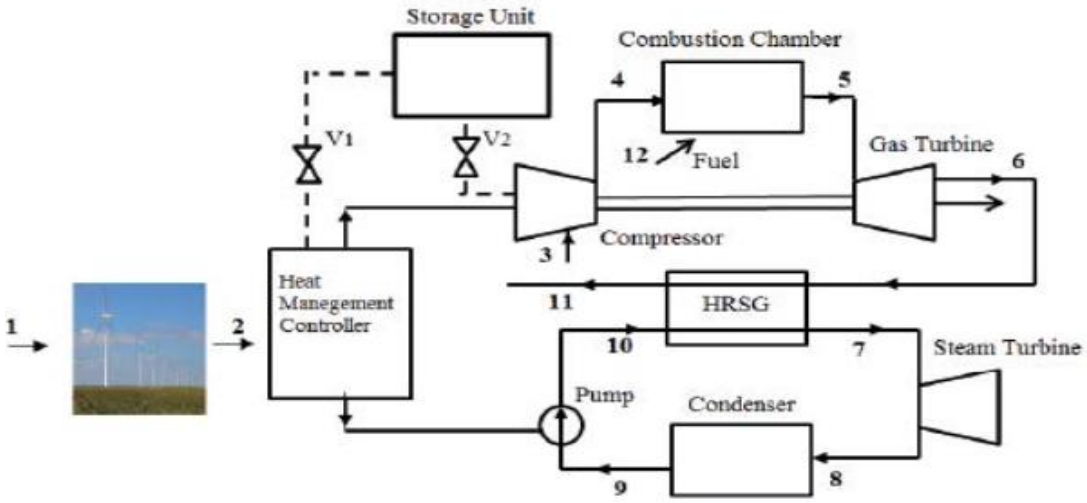

Figure 2. 19. Schematic of the combined cycle with wind turbine [29].

PART 3

SOLUTION METHODOLOGY

Two influential factors (combined cycle and wind turbine) of the developed system merge between a wind turbine and gas-steam combined cycle. The new system is more flexible than a combined cycle alone since WT will provide the power required for the compressor and pump instead of traditional energy from the GT.

3.1. SYSTEM DESCRIPTION AND DISCUSSION SUPPLYING WT REQUIRED POWER FOR GAS-VAPOR COMBINED CYCLE:

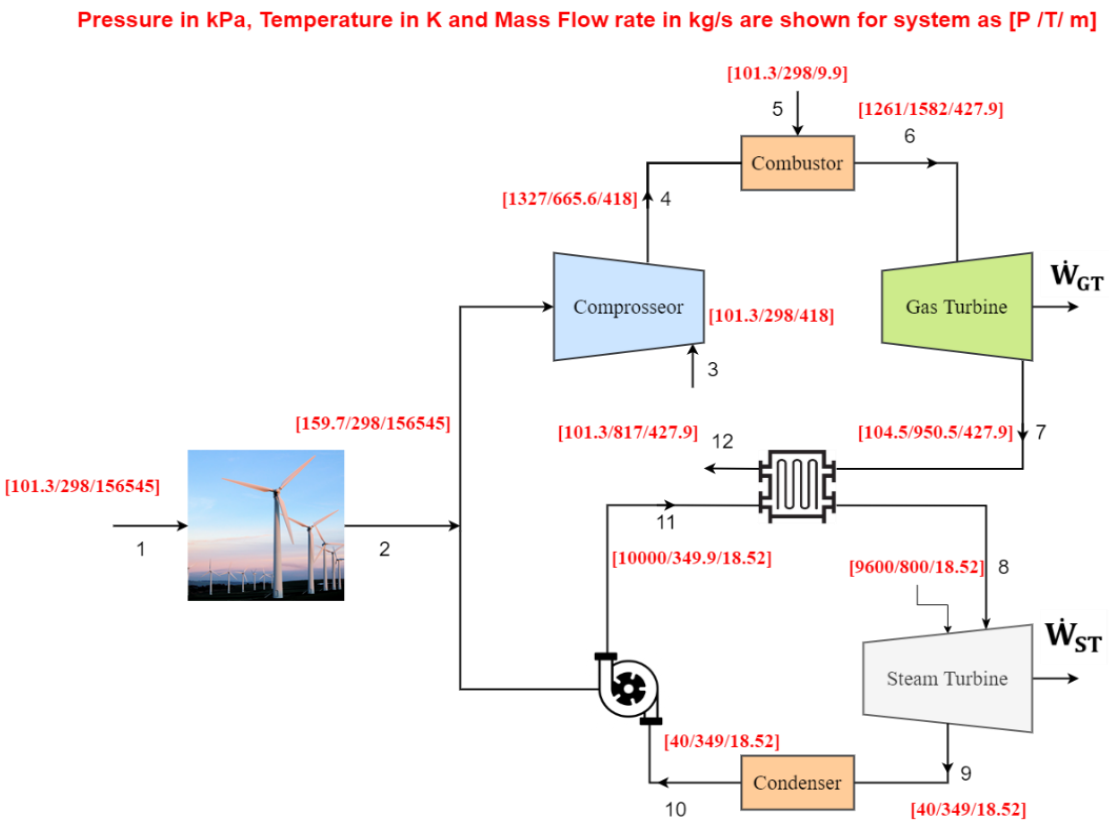

Figure 3. 1. Schematic of WT-GTCC.

The current study is a thermodynamic analysis of a combined cycle (Brayton + Rankine) assisted by a wind turbine. This study also investigates the effect of different operation conditions on the performance of this suggested system.

The compressor in the Brayton cycle and the pump in the Rankine cycle require input power, which is given by the wind turbine when critical wind velocity has been achieved.[29]

As shown in Figure 3. 3, the ambient air at point 3 is compressed in a compressor at a pressure of 0.101 MPa and a temperature of 298.15 K. The compressed air is then introduced into the combustor. At 1.327 MPa, fuel is fed into the combustor. The gas turbine expands the output stream of the combustor, which has a temperature of 1300°C and provides a net power of 333.36 MW. The high temperature and low-pressure exhaust from the Brayton cycle are utilized to power a Rankine cycle. The working fluid is pushed at high pressure in a saturated liquid phase.

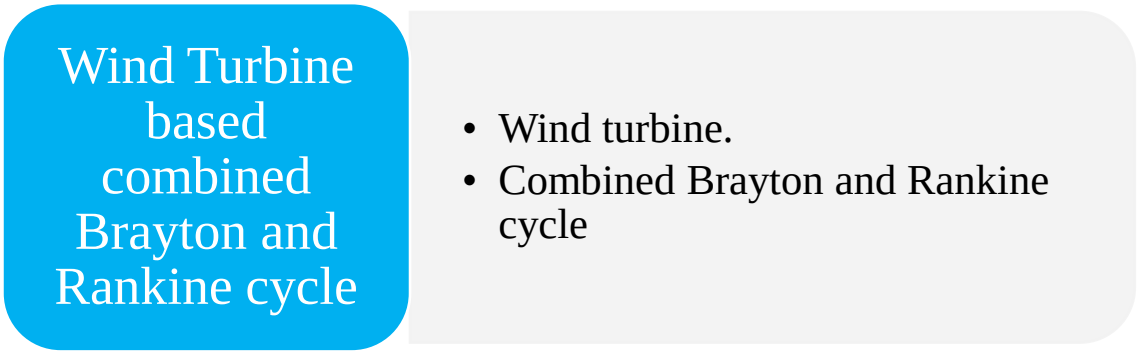

Figure 3. 2. Components of the developed system.

Since WT is the starting point for a developed system that will provide both compressor and the pump with required power, the produced power from wind turbine may be equal, less, and more than that, so must consider that by put controller for energy that comes from wind turbine for these cases:

A. The power of wind turbine power equal to the required power for the compressor and pump will provide the compressor and pump directly (the wind

velocity is equal to the critical speed) by closing the flow valve V2 and the flow valve V1.

B. Power of wind turbine more than required power for compressor and pump the increased power will storage on a storage unit (the wind velocity is more than the critical speed) by the flow valve V2 opens and the flow valve V1 closes, allowing extra power to be stored in the storage unit as compressed air.

C. Power of wind turbine less than required power for compressor and pump the storage power will provide required power the wind velocity is less than the critical speed, and the flow valves V1 are opened, and V2 is closed, allowing extra power in the storage unit to be pumped into the cycle.[1]

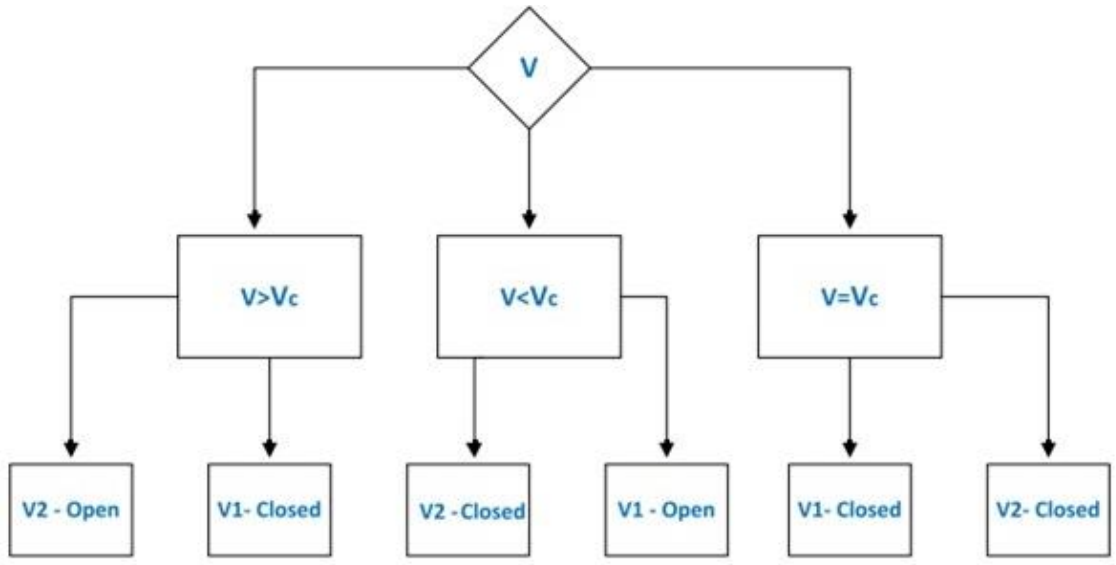

Figure 3. 3. Schematic of flow energy of WT cases [1].

To operate the pump and compressor in the gas-vapor combined cycle without using the energy storage unit or any other inputs, it needs a (minimum) wind velocity. This speed is called the critical velocity. The load demand controls it. (Power of wind turbine equal to required power for compressor and pump the power will provide compressor and pump directly).

When the WT powers the compressor and pump, the net power input to the combined system is as follows:

$$W_{net,input} = W_c + W_p \tag{3.1}$$

When the compressor and pump are powered by the WT and gas/steam turbines produce work, the net power output to the combined system is as follows:

$$W_{net,output} = W_{GT} + W_{ST} + n * W_u - W_C - W_P \tag{3.2}$$

The net power for wind turbine output:

$$W_{net,input} = \sum_{i=1}^{n} n * W_u \tag{3.3}$$

Thermal efficiency provided as [30]:

$$\eta_{th} = \frac{W_{net}}{Q} \tag{3.4}$$

Exergy efficiency is defined as the ratio of output exergy (net exergy work output from the cycle) to input exergy (net exergy work input into the cycle plus exergy entered the fuel injection) [31]:

$$EX_{in\ fuel} = \frac{\dot{m}_{fuel} * ch_{CH4}}{MW_{CH4}} \tag{3.5}$$

$$\Psi_{ex} = \frac{W_{net,output}}{EX_{in\ fuel}} \tag{3.6}$$

3.2. PERFORMANCE AND ANALYSIS OF COMBINED BRAYTON AND RANKINE CYCLE

This section will give the thermodynamic analysis (i.e., first and second law analysis) of the Combined Brayton and Rankine Cycle. The following assumptions will be used in the analysis:

- All components operate in a steady condition, and the kinetic and potential energies terms are negligible.
- Adiabatic heat exchangers.
- The chemical energetic term remains constant throughout the turbine, pumps, compressor, and heat exchanger.
- The temperature and pressure in the surrounding environment are constant (T_0 = 298 K and P_0 = 101.325 kPa).
- Molar flow rates for streams, including any chemical reaction, may be utilized to calculate energy balance equations.
- Air is modeled as an ideal gas having a molar content of 21% oxygen and 79% nitrogen.
- The pump and compressor motors are estimated to have an efficiency of 88 percent.

3.2.1. Compressor Parameter (Process 3-4 Gas)

In the isentropic compression process, the temperature of the air after compression is given by equation 3.8, and the compressor's work demand (in kW) is provided by equation 3.9 [32,33]

$$\dot{m}_3 = \dot{m}_4 \tag{3.7}$$

$$\frac{T_{4s}}{T_3} = \left(\frac{P_4}{P_3}\right)^{\frac{k-1}{k}} \tag{3.8}$$

$$W_C = m_3\, c_p\, (T_4 - T_3) \tag{3.9}$$

$$\dot{m}_3 * S_3 + \dot{S}_{gC} = \dot{m}_4\, S_4 \tag{3.10}$$

$$\dot{m}_3 * EX_3 + W_C = \dot{m}_4 * EX_4 + EXd_{Com} \tag{3.11}$$

$$\eta_{ex,com} = 1 - \left(\frac{EXd_{Com}}{W_c}\right) \tag{3.12}$$

3.2.2. Combustor Parameters (Process 4-6 Gas Fuel)

The methane fuel is used to make the combustor heat transfer heat input in the combustor chamber for theoretical dry air. The complete combustion equation is:

$CH4+A_{th\ (O_2+3{,}76N_2)} = CO2 + 2\,H2O + A_{th}(3.76) + N2$

The balanced combustion equation with EX%/100 excess moist air is:

$CH4+ \quad (1 + EX)A_{th\ (O_2+3{,}76N_2)} = CO2 + 2\,H2O + (1 + Ex)A_{th}(3.76)N2 + Ex(A_{th})O2$

$$m_4 + m_5 = m_6 \tag{3.13}$$

$$m_4\,h_4 + m_5\,h_5 = m_6\,h_6 \tag{3.14}$$

$$m_4\,s_4 + m_5\,s_5 + S_{g.cc} = m_6\,s_6 \tag{3.15}$$

$$m_4 ex_4 + m_5 ex_5 = m_6 ex_6 + Exd_{cc} \tag{3.16}$$

$$\Psi_{ex,cc} = \frac{ex_6 - ex_4}{ex_5} \tag{3.17}$$

Where $ex_5 = ex_{tf} + ex_{ch}$

The chemical exergy of the fuel gases at point 8 can be determined as:

$$y_{co2.dry} = 0.04328\,,\ y_{co2,P} = 0.04101\,,\ y_{H2o,dry} = 0.08656\,,$$
$$y_{H2o,l} = 0.05238\,,\ y_{H2O,P} = 0.08203\,,\ y_{H2O,V} = 0.02964\,,$$
$$y_{N2,dry} = 0.7992\,,\ y_{N2,P} = 0.7575\,,\ y_{o2,dry} = 0.126\,,$$
$$y_{o2,P} = 0.1194\,,\ y_{P,dry} = 0.9476$$

Heat addition in the combustion chamber may be expressed as [34]:

$$Q = \dot{m}_{fuel} * LHV \tag{3.18}$$

3.2.3. Gas Turbine Parameters

During the process of a gas turbine, heated, pressured air gives up its energy by expanding via a turbine. Some of the turbine's output is used to power the compressor when wind turbine energy it's not enough to feed the compressor and pump.

$$m_6 = m_7 \tag{3.19}$$

$$W_{GT} = m_6 c_p (T_6 - T_7) \tag{3.20}$$

$$\dot{m}_6 * S_6 + \dot{S}_{gGT} = \dot{m}_7 S_7 \tag{3.21}$$

$$m_6 ex_6 = W_{GT} + m_7 ex_7 + Exd_{GT} \tag{3.22}$$

$$\frac{T_{7s}}{T_6} = \left(\frac{P_7}{P_6}\right)^{\frac{k-1}{k}} \tag{3.23}$$

$$\eta_{GT} = \frac{(T_6 - T_7)}{(T_6 - T_{7,is})} \tag{3.24}$$

$$\Psi_{ex,GT} = 1 - \frac{Exd_{GT}}{ex_6 - ex_7} \tag{3.25}$$

3.2.4. Heat Recovery Steam Generator Parameters

The expanded air exiting the gas turbine is sent to the heat recovery steam generator (HRSG), where the heat carried by it is used to generate steam. The produced steam is sent to a steam turbine to expand and create steam Rankine cycle output. During the Brayton cycle isobaric process will heat rejection from the air in the atmosphere, during Rankine, the high-pressure liquid enters a heat recovery steam generator and is heated at constant pressure by an external heat source to form a dry saturated vapor.

$$m_7 = m_{12} \tag{3.26}$$

$$m_{11} = m_8 \tag{3.27}$$

$$m_{11} h_{11} + m_7 h_7 = m_8 h_8 + m_{12} h_{12} \tag{3.28}$$

$$m_{11} s_{11} + m_7 s_7 + \dot{S}_{gHRSG} = m_8 s_8 + m_{12} s_{12} \tag{3.29}$$

$$m_{11}ex_{11} + m_7ex_7 = m_8ex_8 + m_{12}ex_{12} + Exd_{HRSG} \quad (3.30)$$

$$\Psi_{ex,HRSG} = \frac{ex_8 - ex_{11}}{ex_7 - ex_{12}} \quad (3.31)$$

3.2.5. Steam Turbine

The dry saturated vapor expands and generates electricity as it passes past a turbine. This reduces the vapor's temperature and pressure, and some condensation may occur. The work output of a steam turbine may be expressed as follows:

$$m_8 = m_9 \quad (3.32)$$

$$W_{ST} = m_8 (h_8 - h_9) \quad (3.33)$$

$$m_8s_8 + \dot{S}_{g,ST} = m_9s_9 \quad (3.34)$$

$$m_8ex_8 = m_9ex_9 + Exd_{ST} + W_{ST} \quad (3.35)$$

$$\eta_{ST} = \frac{(h_8 - h_9)}{(h_8 - h_{9,is})} \quad (3.36)$$

$$\Psi_{ex,ST} = 1 - \frac{Exd_{ST}}{ex_8 - ex_9} \quad (3.37)$$

3.2.6. Condenser

The moist vapor is then condensed at a steady pressure in a condenser to form a saturated liquid and make heat rejection. The heat per unit mass absorbed by the condenser may be calculated as:

$$m_9 = m_{10} \quad (3.38)$$

$$Q_{con} = m_9 (h_9 - h_{10}) \quad (3.39)$$

$$m_9s_9 + \dot{S}_{g,CD} = m_9s_9 + \frac{Q_{con}}{T_0} \quad (3.40)$$

$$\dot{m}_9ex_9 = \dot{m}_{10}ex_{10} + Exd_{CD} \quad (3.41)$$

$$\Psi_{ex,con} = \frac{ex_{10}}{ex_9} \quad (3.42)$$

3.2.7. Pump

The steam is pumped at various pressures ranging from low to high. Because the steam is a liquid at this point, the pump takes less energy to operate through isentropic compression. For an ideal status, the power per unit mass consumed by the pump is provided as:

$$m_{10} = m_{11} \tag{3.43}$$

$$W_P = m_{11}(h_{11} - h_{10}) = \frac{m_{11} * \upsilon_{11}(p_{11} - p_{10})}{\mu_{Pump}} \tag{3.44}$$

$$m_{10}s_{10} + \dot{S}_{g,P} = m_{11}s_{11} \tag{3.45}$$

$$\dot{m}_{10}ex_{10} + W_P = \dot{m}_{11}ex_{11} + Exd_P \tag{3.46}$$

$$\Psi_{ex,P} = 1 - \frac{Exd_P}{W_P} \tag{3.47}$$

3.3. PERFORMANCE AND ANALYSIS OF Wind Energy And (Lanchester–Betz Limit)

The greatest efficiency of the kinetic energy of wind converted to mechanical energy was obtained by Lanchester in 1915 and Betz in 1920 and recorded at the same time its maximum theoretical efficiency. It has been exposed that no wind turbines could convert more than 16/27 of the kinetic energy of wind.[6] The aerodynamics forces generated by the wind produce power output and loads that can produce energy.

3.3.1. Wind Turbine Parameters

The amount of air going through the rotor of a wind turbine per unit time is used to calculate the available power. Equation (3.48) is used to calculate the mass flow rate of the air stream hitting the rotor surface ($A = \pi R^2$) where R is the rotor radius its 65 m (SWT-DD-130 Siemens [35]). Using T_0 = 25 C and p_0 = 0.101 MPa as the reference

temperature and pressure of the environment and air density = 1.18 kg/m^3, the mass flow rate is [29]:

$$\dot{\mathbf{m}} = \boldsymbol{\rho \mathbf{A} \mathbf{v}_r} \tag{3.48}$$

Equation (3.49) is used to calculate available power [36] :

$$W_a = mk_e = \frac{\rho A v_r^3}{2} \text{ (Maximum theoretical work)} \tag{3.49}$$

$$\frac{p_1}{\rho} + \frac{V_1^2}{2} = \frac{p_2}{\rho} + \frac{V_2^2}{2} \tag{3.50}$$

$$\dot{m}_1 \left(h_1 + \frac{V_1^2}{2}\right) = \dot{m}_2 \left(h_2 + \frac{V_2^2}{2}\right) + \dot{W}_{WT} \tag{3.51}$$

For entropy and exergy of a wind turbine, it can calculate as follows:

$$\dot{m}_1 * S_1 + \dot{S}_{gWT} = \dot{m}_1 S_2 \tag{3.52}$$

$$\dot{m}_1 \left(EX_1 + \frac{V_1^2}{2}\right) = \dot{m}_2 \left(EX_2 + \frac{V_2^2}{2}\right) + \dot{W}_{WT} + EXd_{WT} \tag{3.53}$$

Equation (3.54) is used to determine exit velocity [29]:

$$V_2 = \frac{\omega * R}{V_1} \tag{3.54}$$

where ω (rad/sec) is the angular velocity of the turbine

C_p denotes the proportion of upstream wind power collected by the rotor blades denotes proportion of upstream wind power collected by the rotor blades also known as the Betz limit. This number is also known as the rotor power coefficient or rotor efficiency. The power coefficient does not have a fixed value. It fluctuates with the wind turbine's tip speed ratio. Even in the best-designed wind turbines, values of 0.35-0.45 are frequent in the actual world, much below the Betz limit [37]. According to the Betz criteria, the maximum value of Cp is 0.5926 (in current research, it's 0.5).

Equation (3.55) [29]. gives the power coefficient in this analysis, the losses of electrical and mechanical equipment were estimated to be μ alternator = μ mechanic = 0.97.

$$C_P = \frac{W_e}{\mu_{alternator} * \mu_{mechanical} * 0.5 * \rho * \pi * R^2 * v_r^3} \quad (3.55)$$

Wind turbine exergy efficiency is defined as a measure of how well fluid flow exergy is converted into helpful turbine or inverter work. Exergy efficiency is obtained from Equation (3.56) [29]:

$$\Psi_{WT} = \frac{W_e}{W_u} = \frac{W_e}{E_1 - E_2} \quad (3.56)$$

3.3.2. Turbine Blade Design (Tip Speed Ratio) Effect

The tip speed ratio is defined as the relationship between the rotor blades' velocity and the wind's velocity. Equation (3.57) is the primary design parameter around which all other optimal rotor dimensions are calculated [3]:

$$\lambda = \frac{\Omega * R}{V_{wind}} \quad (3.57)$$

Consideration should be given to a variety of criteria when establishing the ideal speed for the tip of the blade, as shown in Table 3. 1. Higher tip speeds can boost a turbine's efficiency [29], albeit the gain is negligible when other factors such as increased noise, aerodynamic and centrifugal stress are considered.

Table 3. 1. Design considerations for tip speed ratios [3].

Tip Speed Ratio	Low	High
Value	Low tip speeds range from one to two.	Tip Speeds greater than 10 are considered fast.

Utilization	conventional windmills and water pumps	Prototypes are mostly single or two-bladed.
Torque	Increases	Decreases
Performance	Reduces significantly below five because to the rotating wake produced by high torque.	Increases are insignificant after eight years.
Centrifugal Stress	Decreases	As a square of rotational velocity, it rises.
Aerodynamic Stress	Decreases	Increases in proportion to the rotational velocity
Solidity Area	Increasingly, several 20+ blades are necessary.	Decreases significantly
Profile of the Blade	Large	Significantly Limited
Aerodynamics	Simple	Critical

A faster tip speed necessitates narrower chord widths, resulting in narrower blade profiles. This can result in cheaper material utilization and production costs. However, higher tip speeds are related to increased centrifugal and aerodynamic forces. The increasing pressures indicate that preserving structural integrity and preventing blade failure are demanding tasks. The aerodynamics of the blade design become increasingly important as the tip speed increases. A blade built for high relative wind velocity produces less torque at lower speeds. As a result, there is a more significant reduction in speed [36]and difficulties in self-starting. Increased tip speeds are also related to an increase in noise since noise increases nearly proportionally to the sixth power [3,38].

PART 4

RESULTS AND CONCLUSION

2.5. INPUT PARAMETERS

The data of a Wind turbine (SWT-DD-130 Siemens) and gas turbine (GE 9E.03) were used to simulate a wind-assisted combined cycle. The Engineering Equation Solver software (EES) was used to acquire the findings. Table 4.1 lists the main input parameters and assumptions values during the simulation.

Table 4. 1. Main input parameters and assumptions values during the simulation.

Parameter	**Values**
Wind Velocity	10 m/s
Blade radius SWT-DD-130 Siemens	65 meters [35]
Compressor inlet air temperature	273 [K]
Compressor inlet air Pressure	101 [kPa]
Pressure Ratio (GE 9E.03)	13.1 [39]
Lower heating value of the fuel (methane)	50.05 MJ/kg
Isentropic efficiency of Compressor	88%
Isentropic efficiency of Pump	88%
Isentropic efficiency of Gas Turbine	92%
Isentropic efficiency of Steam Turbine	92%
Steam inlet pressure of heat recovery steam generator	10,000 [kPa] [39]
Steam outlet temperature of heat recovery steam generator	817 [K] [39]
Mass flow rate of fuel	9.9 kg/sec [39]
Mass flow rate of air	418 kg/sec [39]
Pressure drops in gas combustion chamber	5%

Pressure drops in the heat recovery steam generator (gas side)	3%
Pressure drops in the heat recovery steam generator (steam side)	4%

2.6.VALIDATION

Table 4. 2 shows validation of the combined cycle model in this study with the data sheet of the gas turbine GE 9E.03 [39]. The comparison presents that the results between them are close, and the difference is minimal. It is clear from Table 4. 2 that the developed model of this study produces 193.38 MW while the data sheet of GE 9E.03 gas turbine in combined cycle produces 204 MW.

Table 4. 2. Validation of the combined cycle model with the gas turbine GE 9E.03 [39].

Parameter	**GE 9E.03 Model**	**Present model**
Pressure ratio	13.1	13.1
Net Output (MW)	204	193.38
Mass flow rate of fuel (kg/s)	9.9	9.9
Mass flow rate of air (kg/s)	418	418
Gas turbine generator type	Air	Air

Table 4-3 shows validation of the wind turbine model used in this study with the manufactured company's wind turbine SWT-DD-130 Siemens data sheet [35]. The findings show that the wind turbine in this study produces 3.68 MW, whereas the date range of the power produced by SWT-DD-130 Siemens is 3.55-4.3 MW.

Table 4. 3. Validation of the wind turbine model with the wind turbine SWT-DD-130 Siemens [35].

Parameter	**SWT-DD-130 Siemens**	**Present model**
Flexible power rating (MW)	3.55-4.3	3.68
Diameter (meter)	130	130
Swept area (m^2)	13,300	13,267
Standard operating temperature	from -20ºC to 40ºC	25 ºC

2.7. RESULTS PARAMETERS

Table 4. 4 displays the thermodynamic characteristics such as enthalpy, entropy, mass flow rate, temperature, pressure, and exergy for each state of the WT-GTCC under optimum operating circumstances.

Table 4. 4. The properties for each state for the WT-GTCC at the optimum condition

State	T (K)	P (kPa)	h (kJ/kg)	s (kJ/kg-K)	m (kg/s)	X (MJ)
1	298	101.3	298.4	5.694	156545	7.75
2	298	159.7	298.4	5.694	156545	3.68
3	298	101.3	298.4	5.694	418	159.1
4	665.6	1327	676.7	5.779	418	147.6
5	298	101.3	-4650	11.61	9.9	513.2
6	1582	1261	264.5	8.266	427.9	519.7
7	950.5	104.5	-536.5	8.354	427.9	165.7
8	800	9600	3448	6.71	18.52	28.39
9	349	40	2393	6.973	18.52	7.403
10	349	40	317.6	1.026	18.52	1.802
11	349.9	10000	329.2	1.03	18.52	1.995
12	817	101.3	-695.3	8.183	427.9	119.6

Table 4. 5 reveals the performance for each component of GTCC and WT-GTCC cycles. The Table presents the GTCC produces 193.38 MW while the WT-GTCC

produces 355.4 MW when wind velocity is 10 m/s for 44 wind turbine units. It is shown in Table 4. 5 that for the GTCC cycle, the η_{exerg} and $\eta_{thermal}$ are 37.68 percent and 39.42 percent, respectively, but for the WT-GTCC cycle, they rise to 69.25 percent and 72.44 percent as a result of the addition of wind turbines to the cycle.

Table 4. 5. Energy performance for each component of GTCC and WT-GTCC cycles

	WT-GTCC	**GTCC**
Work output from the gas turbine (MW)	333.364	333.364
Work input for air compressor (MW)	159.1	159.1
Work net from Brayton cycle (BC) (MW)	174.265	174.265
Work output from ST (MW)	19.332	19.332
Work input to the pump (MW)	0.22	0.22
Work net from (Rankine cycle) RC (MW)	19.113	19,113
Work output from the wind turbine (44 unit) (MW)	162.008	0
Net output power (MW)	355.401	193.38
Overall exergy efficiency (%)	69.25	37.68
Overall thermal efficiency (%)	72.44	39.42

The main exergy analysis results for a different part of the GTCC are presented in Table 4.6 and Figure 4.1. As demonstrated in this Table, the detailed data of inlet, outlet, and destruction exergies can be found for each part of the cycle. This Table also shows the details of $\dot{X}_d$% and exergy efficiency for each component. Concerning Table 4.6 and Figure 4.1, it shows that the most exergy destruction of the GTCC components related to the combustion chambers is 141.1MW because of the more of irreversibility for a chemical reaction (70.46 % of the $\dot{X}_d$ is destroyed through the CC). The gas turbine comes next with a 20.58 MW exergy destruction (10.3 % of the $\dot{X}_d$ is destroyed through the GT).

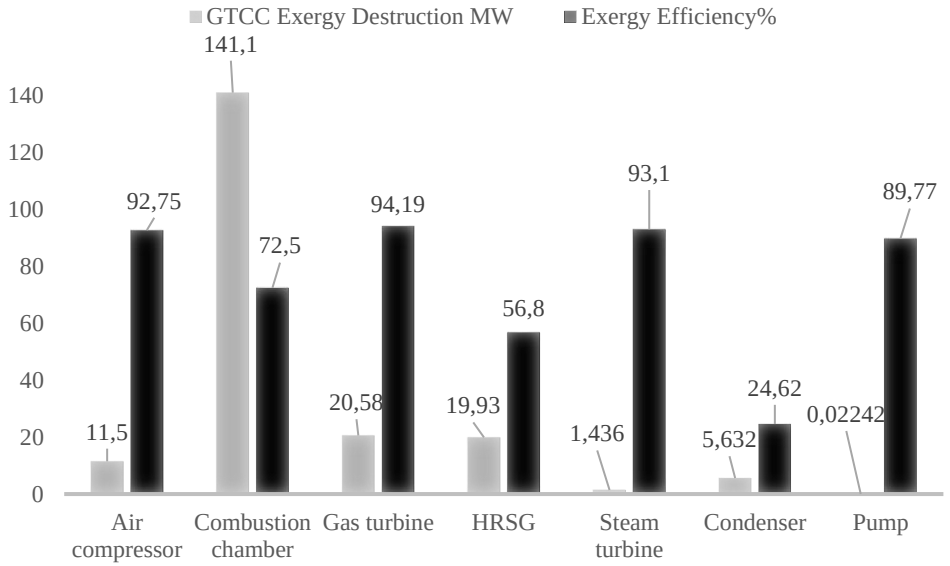

Figure 4. 1. Exergy analysis of the power plant at GTCC

Table 4. 6. Exergy analysis for each component of GTCC

Component	$\dot{X}_{input}$ (MW)	$\dot{X}_{output}$ (MW)	$\dot{X}_{destruction}$ (MW)	$\dot{X}_{destruction}$ (%)	Exergy efficiency (%)
Air compressor	159.1	147.6	11.53	5.75	92.75
Combustion chamber	660.8	519.7	141.1	70.46	72.5
Gas turbine	519.7	165.7	20.58	10.27	94.19
HRSG	167.736	147.84	19.93	9.95	56.8
Steam turbine	28.24	7.471	1.436	0.71	93.1
Condenser	7.471	1.839	5.632	2.8	24.62
Pump	1.839	2.036	0.02242	0.01	89.77
GTCC	1544.886	992.186	200.23	100	37.68

Figure 4.2 Table 4.7 present the exergy analysis for each component of WT-GTCC cycles. It illustrated from the results that the most exergy destruction of the WT-GTCC cycle components connected to the WT is 179 MW (47.2% of the $\dot{X}_d$ is destroyed

through the WT in the WT-GTCC cycle). The CC and GT come next with 141.1 MW and 20.58 MW exergy destruction rates (37.21% and 5.42% of the $\dot{X}_d$ is destroyed through the CC and GT). The Table also presented that the maximum exergy efficiency related to the GT (94.19 %).

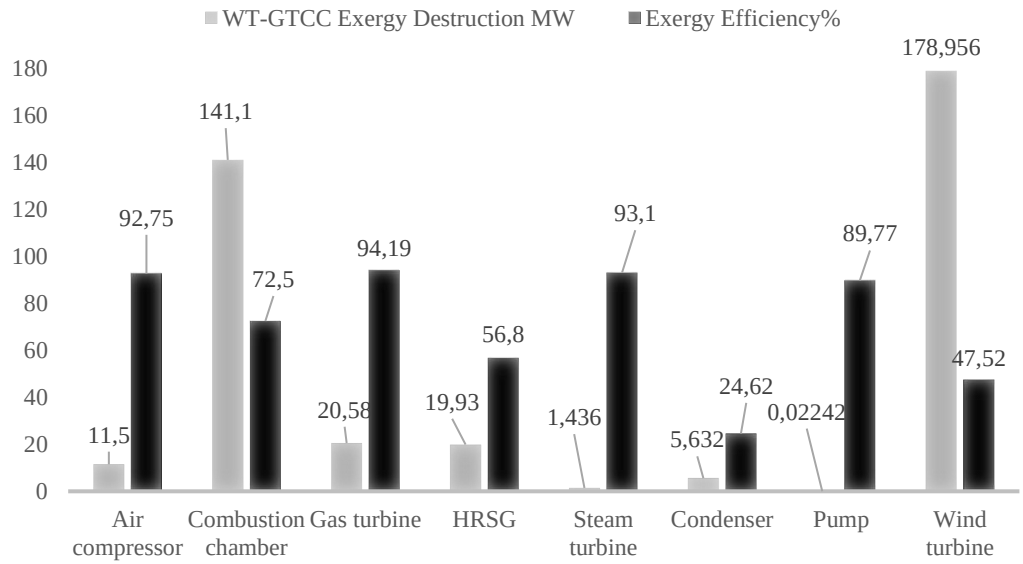

Figure 4. 2. Exergy analysis of the power plant at WT-GTCC

Table 4. 7. Exergy analysis for each component of WT- GTCC

Component	$\dot{X}_{input}$ (MW)	$\dot{X}_{output}$ (MW)	$\dot{X}_{destruction}$ (MW)	$\dot{X}_{destruction}$ (%)	Exergy efficiency (%)
Air compressor	159.1	147.6	11.5	3.03	92.75
Combustion chamber	660.8	519.7	141.1	37.21	72.5
Gas turbine	519.7	165.7	20.58	5.42	94.19
HRSG	167.736	147.84	19.93	5.25	56.8
Steam turbine	28.24	7.471	1.436	0.37	93.1
Condenser	7.471	1.839	5.632	1.48	24.62
Pump	1.839	2.036	0.02242	0.006	89.77
Wind turbine	340.956	162	178.956	47.2	47.52
WT-GTCC	1885.837	1154.18	379.186	100	69.25

2.8. RESULTS DISCUSSING AND IMPROVING

Figure 4.3-4.6 show the impact of wind velocity on the WT-GTCC and the GTCC's performance. Figures 4.3 present that the $\dot{W}_{net}$ of the WT-GTCC cycle is greater than the $\dot{W}_{net}$ of the GTCC cycle due to the power produced by the wind turbine. It's also clear from this figure that the $\dot{W}_{net}$ of the GTCC cycle remains 193.38 MW while the $\dot{W}_{net}$ of the WT-GTCC cycle increases from 194.675 to 473.353 MW as the wind velocity increases from 2 to 12 m/s.

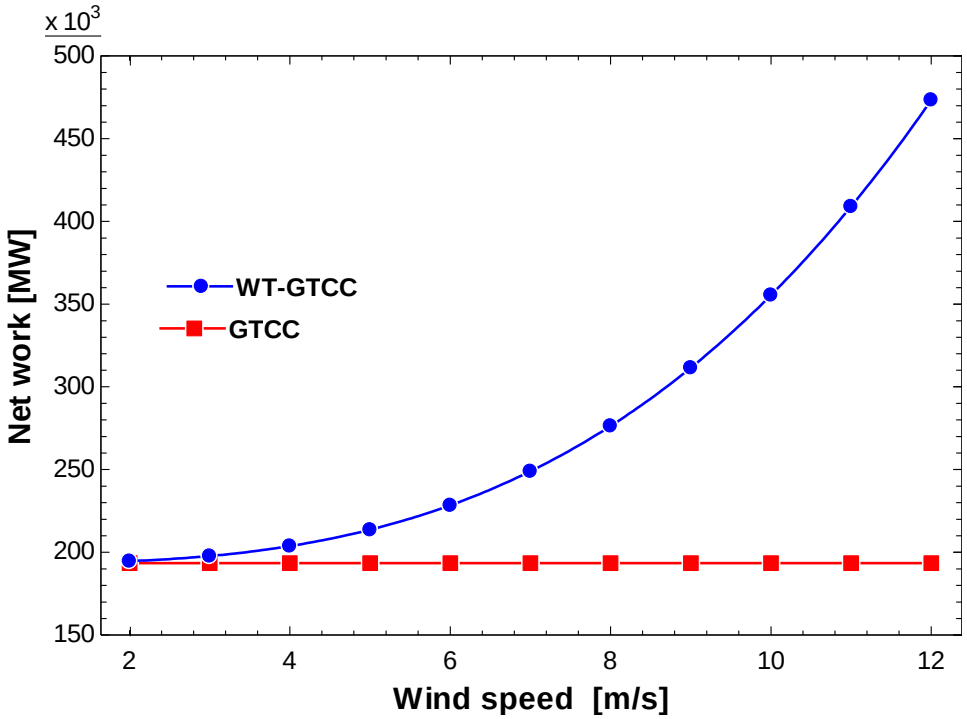

Figure 4. 3. Compares the work net of each WT-GTCC and GTCC cycle affected by the wind velocity

Figure 4. 4 reveals the effect of the wind velocity on the η_{themal} of both cycles. The finding presents that the η_{themal} of the GTCC cycle doesn't affect by the change in wind velocity because the $\dot{W}_{net}$ of the GTCC cycle remains constant. In contrast, the η_{themal} of the WT-GTCC enhances with the wind velocity increase because of the wind turbine's power. When wind speed rises from 2 to 12 m/s, the WT-GTCC cycle's thermal efficiency goes up to 96.48 percent, while the η_{themal} for the GTCC cycle stays constant at 39.42 percent, according to the graphs.

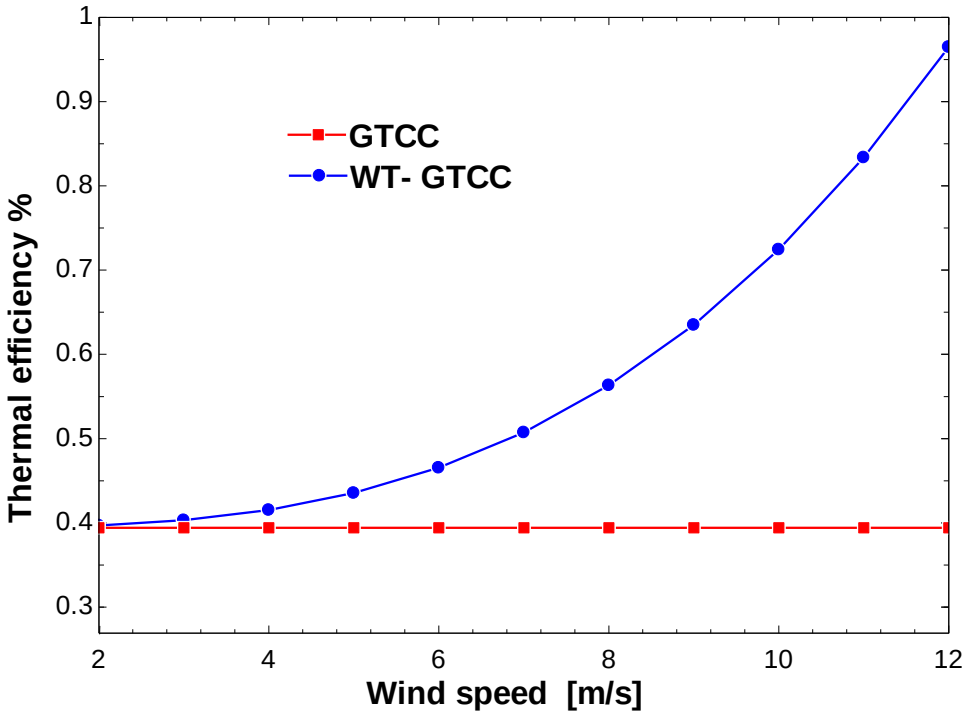

Figure 4. 4. Compares the thermal efficiency of each WT-GTCC and GTCC cycle affected by the wind velocity

Figure 4. 5 reveals the effect of the wind velocity on the mass flow rate of wind and usable work for each unit of a wind turbine. According to the findings, the mass flow rate of wind rises along with an increase in wind velocity due to a rise in the speed across the blades. Also, usable work will increase due to the effect velocity directly in usable work according to equation (3.8). The curves presented that the mass increases from 31,309 to 187,854 kg/s with the rise of the wind velocity from 2 to 12 m/s, and the usable work for each unit of a wind turbine in the cycle will increase from 0.02946 to 6.363 MW.

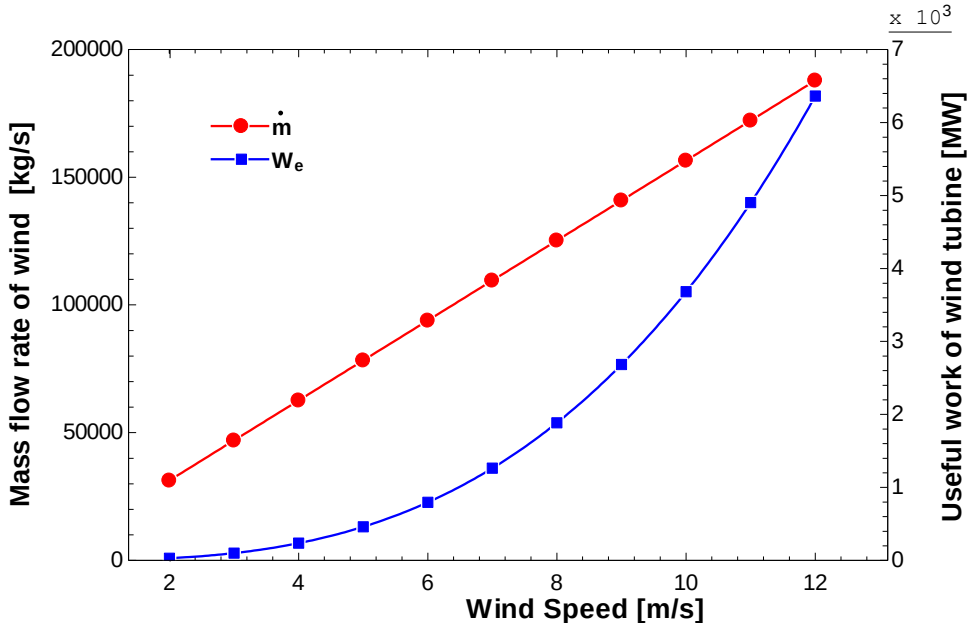

Figure 4. 5. Depicts wind velocity's effect on wind turbine useable energy and mass flow rate.

Figure 4. 6 reveals the effect of the wind velocity on WT exergy efficiency and maximum theoretical work. Figure 4.6 presents that the exergy efficiency drops when wind speed increases because the quantity of kinetic energy that can be transferred to productive work is reduced.

The results revealed that when the wind velocity increases from 2 to 12 m/s, the useful work of wind turbine increase from 0.02946 to 6.363 MW, but theoretical work increases from 0.047 to 13.432 MW. The increasing in the difference between useful and theoretical works makes a reduction in the exergy efficiency of wind turbine. The curves show that the wind turbine's exergy efficiency decreases from 62.73 to 47.37 percent.

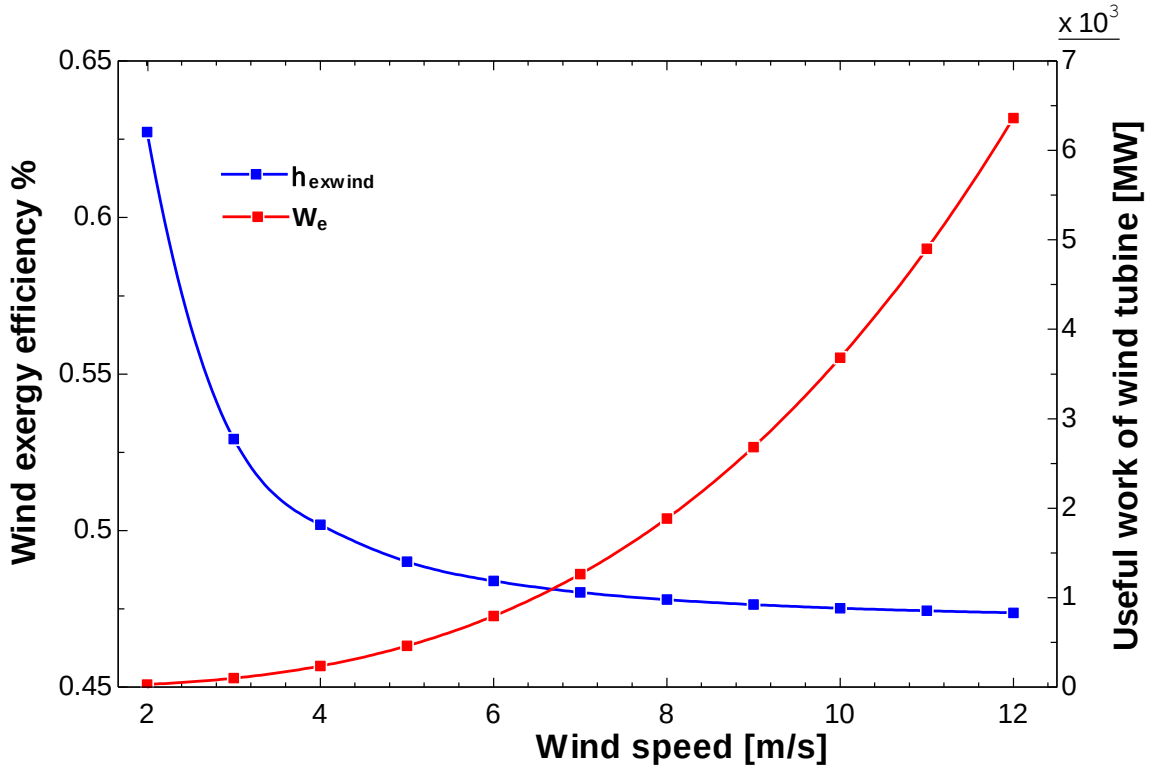

Figure 4. 6. Influence of wind velocity on WT's exergy efficiency and useful work.

Figure 4. 7 reveals the effect of the blade radius of the wind turbine on the Ẇnet of the WT-GTCC cycle and the useful work of each wind turbine at wind velocity fixed at 10 m/s. The findings present that the $\dot{W}_{net}$ of the WT-GTCC increase by increasing the blade radius due to increasing the amount of useful work of each wind turbine unit due to the rise in the surface of the wind turbine that picks the wind (radius blade of the wind turbine). The curves presented that the $\dot{W}_{net}$ increases from 289.25 MW to 438.81 MW for the WT-GTCC cycle, and the useful work of each wind turbine increases from 2.179 to 5.578 MW with the rise of the blade radius from 50 to 80 m.

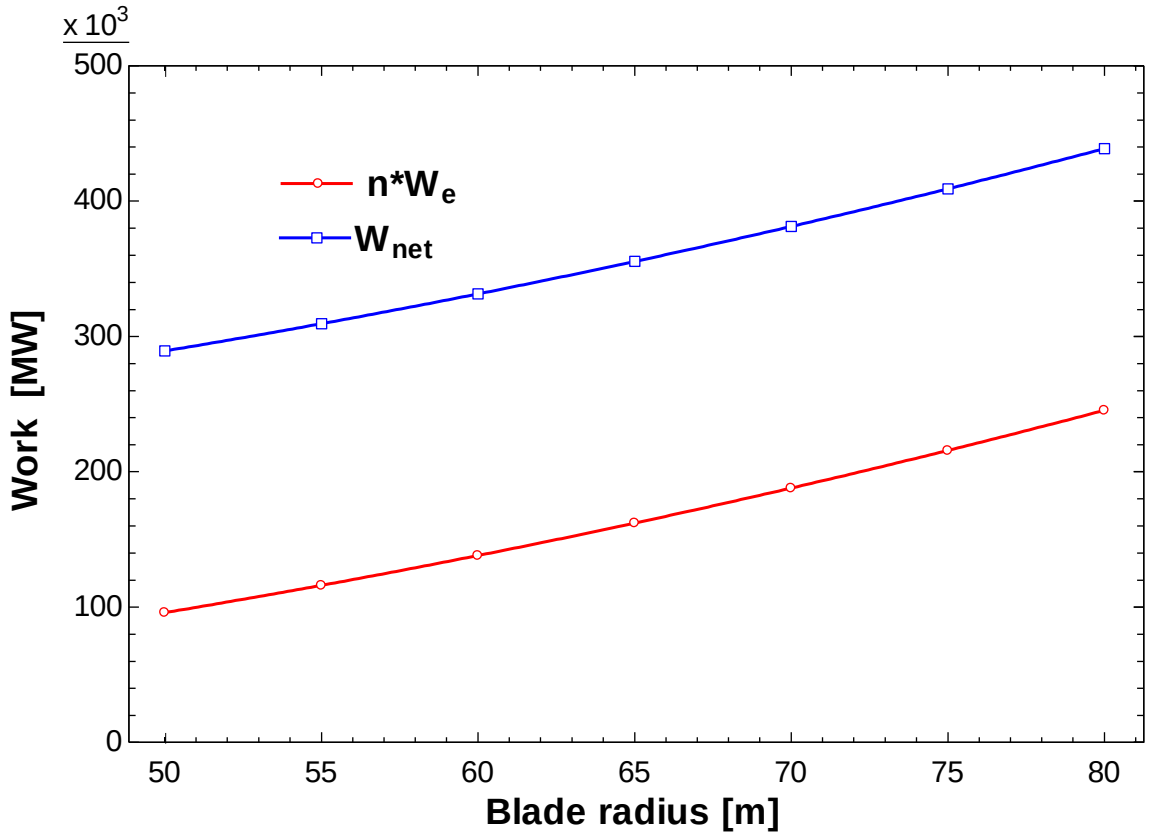

Figure 4. 7. Effect radius of wind turbine blades on useful work for wind turbine and work net of WT-GTCC.

PART 5

CONCLUSION AND RECOMMENDATION

5.1. CONCLUSION

This study purpose that it is conceivable to work on a wind-assisted combined power plant using wind turbines and a combined cycle (Brayton + Rankine) to increase total energy by roughly 45.2% by supplying compressor and pump power from wind turbine energy.

It is preferable to concentrate on selecting wind turbines and gas turbine types since it has a significant impact on net energy.

as shown in the findings, since can calculate required power for compressor and pump 159.318 MW, it can calculate critical wind velocity for a 44-unit wind turbine its 9.944 m/s may entirely cover the energy of the compressor and pump.

This study's key findings may be summarized as follows:

1. Rise wind velocity in the wind turbines improved the system's performance.
2. Thermal and energy analysis is the best design and performance evaluation tool for generating energy.
3. Choosing the pressure rate for the compressor (GE.9E 03) was very appropriate, as shown in the results and diagrams. There was an increase in the energy produced when the pressure rate was increased.
4. Choosing the radius of blades 65 meters SWT-DD-130 Siemens was very appropriate, as shown in the results and diagrams. More than this radius will need a very high column to save blades from hitting the ground and make it harder to manufacture.
5. The $\dot{W}_{net}$ of the WT-GTCC cycle is greater than the $\dot{W}_{net}$ of the GTCC cycle due to the power produced by the wind turbine.

6. The work net produced by the GTCC is 193.38 MW, while it has 355.4 MW for WT-GTCC when wind velocity is ten m/s for 44 wind turbine units
7. WT-GTCC is 355.4 MW; its thermal and exergy efficiencies were 71.89 percent and 68.72 percent, respectively.
8. The results showed that the maximum exergy losses occur in the wind turbine and combustor chamber for WT-GTCC.
9. for the GTCC cycle, the η_{exerg} and $\eta_{thermal}$ are 37.68 percent and 39.42 percent, respectively, but for the WT-GTCC cycle, they rise to 69.25 percent and 72.44 percent as a result of the addition of wind turbines to the cycle.
10. The $\dot{W}_{net}$ of the WT-GTCC increase by increasing the blade radius due to the rise in the surface of the wind turbine that picks the wind (radius blade of the wind turbine).

5.2. RECOMMENDATION

Some key concerns that were not addressed in the prior literature or this thesis developed because of this study on wind turbines and combined cycles (Brayton and Rankine), and they are relevant to this study and can be worked on in the future.

It is possible to know the critical speed that leads to saving the entire energy produced from the gas and steam turbines because the amount of energy required for the compressor and pump can be calculated through the equations (3.13), (3.48) and it is decided to use 44-units of the wind turbine, so the critical speed is 9.944 meters per second, therefore including this combination between the combined cycle (Brayton and Rankine) and the wind turbine greatly improves the overall efficiency and the amount of energy produced.

REFERENCES

1. Rabbani, M., Dincer, I., and Naterer, G. F., "Thermodynamic assessment of a wind turbine based combined cycle", ***Energy***, 44 (1): 321–328 (2012).

2. "How a Wind Turbine Works - Text Version | Department of Energy", **https://www.energy.gov/eere/wind/how-wind-turbine-works-text-version** (2022).

3. Schubel, P. J. and Crossley, R. J., "Wind Turbine Blade Design", 5: 3425–3449 (2012).

4. "Wind Energy | EcoPlanet Energy", **http://ecoplanetenergy.com/all-about-eco-energy/overview/wind/** (2022).

5. Habali, S. M. and Saleh, I. A., "Local design, testing and manufacturing of small mixed airfoil wind turbine blades of glass fiber reinforced plastics. Part I: design of the blade and root", ***Energy Conversion And Management***, 41 (3): 249–280 (2000).

6. Wagner, H.-J., Monastero, V., and Univ-Prof H-J Wagner, C., "International School on Energy “New Strategies for Energy Generation, Conversion and Storage” Introduction to wind energy systems Content P a g e N o", .

7. McCormick, B. W., "Helicopters", ***Encyclopedia Of Physical Science And Technology***, 309–320 (2003).

8. "THERMODYNAMICS: AN ENGINEERING APPROACH (Eight Edition) - YUNUS A. ÇENGEL - MİCHAEL A. BOLES | Nadir Kitap", **https://www.nadirkitap.com/thermodynamics-an-engineering-approach-eight-edition-yunus-a-cengel-michael-a-boles-kitap23212088.html** (2022).

9. "8.7 Combined Cycles for Power Production", **https://web.mit.edu/16.unified/www/FALL/thermodynamics/notes/node67.html** (2022).

10. Ghosh, T. K. and Prelas, M. A., "Energy Resources and Systems", Energy Resources and Systems, ***Springer***, [Dordrecht], 1–778 (2009).

11. "Form EIA-860 Detailed Data with Previous Form Data (EIA-860A/860B)", **https://www.eia.gov/electricity/data/eia860/** (2022).

12. McGowan, "Wind Energy Explained, Theory, Design and Application", 688 (2009).

13. Golecha, K., Eldho, T. I., and Prabhu, S. V., "Influence of the deflector plate on the performance of modified Savonius water turbine", ***Applied Energy***, 88 (9): 3207–3217 (2011).

14. Mohamed, M. H., Janiga, G., Pap, E., and Thèvenin, D., "Optimization of Savonius turbines using an obstacle shielding the returning blade", ***Renewable Energy***, 35 (11): 2618–2626 (2010).
15. Altan, B. D., Atilgan, M., and Özdamar, A., "An experimental study on improvement of a Savonius rotor performance with curtaining", ***Experimental Thermal And Fluid Science***, 32 (8): 1673–1678 (2008).

16. Crawford, R. H., "Life cycle energy and greenhouse emissions analysis of wind turbines and the effect of size on energy yield", ***Renewable And Sustainable Energy Reviews***, 13 (9): 2653–2660 (2009).

17. Pope, K., Dincer, I., and Naterer, G. F., "Energy and exergy efficiency comparison of horizontal and vertical axis wind turbines", ***Renewable Energy***, 35 (9): 2102–2113 (2010).

18. Hall, J. F. and Chen, D., "Performance of a 100 kW wind turbine with a Variable Ratio Gearbox", ***Renewable Energy***, 44: 261–266 (2012).

19. Kumar, A. and Stol, K., "Simulating feedback linearization control of wind turbines using high-order models", ***Wind Energy***, 13 (5): 419–432 (2010).

20. Shen, X., Zhu, X., Energy, Z. D.-, and 2011, undefined, "Wind turbine aerodynamics and loads control in wind shear flow", ***Elsevier***, .

21. Khaliq, A. and Kaushik, S. C., "Second-law based thermodynamic analysis of Brayton/Rankine combined power cycle with reheat", ***Applied Energy***, 78 (2): 179–197 (2004).

22. Khaljani, M., Khoshbakhti Saray, R., and Bahlouli, K., "Comprehensive analysis of energy, exergy and exergo-economic of cogeneration of heat and power in a combined gas turbine and organic Rankine cycle", ***Energy Conversion And Management***, 97: 154–165 (2015).

23. Marrero, I. O., Lefsaker, A. M., Razani, A., and Kim, K. J., "Second law analysis and optimization of a combined triple power cycle", ***Energy Conversion And Management***, 43 (4): 557–573 (2002).
24. Ahmadi, P., Dincer, I., and Rosen, M. A., "Exergy, exergoeconomic and environmental analyses and evolutionary algorithm based multi-objective optimization of combined cycle power plants", ***Energy***, 36 (10): 5886–5898 (2011).

25. Cihan, A., Hacihafizoğlu, O., and Kahveci, K., "Energy–exergy analysis and modernization suggestions for a combined-cycle power plant", ***International Journal Of Energy Research***, 30 (2): 115–126 (2006).

26. Nag, P. K. and Raha, D., "Thermodynamic analysis of a coal-based combined cycle power plant", ***Heat Recovery Systems And CHP***, 15 (2): 115–129 (1995).

27. Ibrahim, T. K., Rahman, M. M., and Abdalla, A. N., "Gas Turbine Configuration for Improving the performance of Combined Cycle Power Plant", ***Procedia Engineering***, 15: 4216–4223 (2011).

28. Bassily, A. M., "Modeling, numerical optimization, and irreversibility reduction of a dual-pressure reheat combined-cycle", ***Applied Energy***, 81 (2): 127–151 (2005).

29. Sheykhlou, H., "Thermodynamic Analysis of a Combined Brayton and Rankine Cycle based on Wind Turbine", ***Journal Of Fundamentals Of Renewable Energy And Applications***, 06 (02): (2016).

30. Akroot, A., "Effect of Operating Temperatures on the Performance of a SOFCGT Hybrid System", ***International Journal Of Trend In Scientific Research And Development***, Volume-3 (Issue-3): 1512–1515 (2019).

31. Akroot, A. and Nadeesh, A., "Performance Analysis of Hybrid Solid Oxide Fuel Cell-Gas Turbine Power System", (2021).

32. Alam, K. and Dubey, M. K. K., "PERFORMANCE ANALYSIS OF COMBINED GAS TURBINE-STEAM TURBINE POWER GENERATION CYCLE BACHELOR OF TECHNOLOGY IN MECHANICAL ENGINEERING", (1614).

33. Akroot, A. and Namli, L., "Performance assessment of an electrolyte-supported and anode-supported planar solid oxide fuel cells hybrid system", ***J Ther Eng***, 7 (7): 1921–1935 (2021).

34. Akroot, A., Namli, L., and Ozcan, H., "Compared Thermal Modeling of Anode- and Electrolyte-Supported SOFC-Gas Turbine Hybrid Systems", ***Journal Of Electrochemical Energy Conversion And Storage***, (2021).

35. Internet: Siemens Gamesa, "Siemens Gamesa Data Sheets SWT-DD-130", **https://www.siemensgamesa.com/en-int/-/media/siemensgamesa/downloads/en/products-and-services/onshore/data-sheets/siemens-gamesa-onshore-wind-turbine-swt-dd-130-en.pdf** (2022).

36. Yurdusev, M. A., Ata, R., and Çetin, N. S., "Assessment of optimum tip speed ratio in wind turbines using artificial neural networks", ***Energy***, 31 (12): 2153–2161 (2006).

37. Manyonge, A. W., Manyala, R., Shichika, J., Manyonge, A. W., Ochieng, R. M., Onyango, F. N., and Shichikha, J. M., "Mathematical modelling of wind turbine in a wind energy conversion system: Power coefficient analysis", ***Applied Mathematical Sciences***, 6 (91): 4527–4536 (2012).

38. Duquette, M. M. and Visser, K. D., "Numerical Implications of Solidity and Blade Number on Rotor Performance of Horizontal-Axis Wind Turbines", ***Journal Of Solar Energy Engineering***, 125 (4): 425–432 (2003).

39. Internet: GE Gas Power, "9E Gas Turbine (50 Hz) | 9E.03/9E.04 Gas Turbine | GE Gas Power", **https://www.ge.com/gas-power/products/gas-turbines/9e** (2022).

RESUME

Hasan Yassin entered Karabuk University in 2015 as a bachelor’s degree student in the mechanical engineering department and graduated from it in 2019 with a 2.99 GPA. He then worked as a mechanical design engineer at the Smartmak Makine company during 2019-2021 And continues his career in Zartaşa company as Project engineer position. He joined the master's degree in Karabuk University in 2019.